นาโนคอมพอสิตฟิล์มที่เป็นเซลลูโลสทั้งหมดจากเส้นใยป่านศรนารายณ์

นายนพพล สมเศรษฐ์

จุฬาลงกรณ์มหาวิทยาลัย
Chulalongkorn University

บทคัดย่อและแฟ้มข้อมูลฉบับเต็มของวิทยานิพนธ์ตั้งแต่ปีการศึกษา 2554 ที่ให้บริการในคลังปัญญาจุฬาฯ (CUIR)
เป็นแฟ้มข้อมูลของนิสิตเจ้าของวิทยานิพนธ์ ที่ส่งผ่านทางบัณฑิตวิทยาลัย
The abstract and full text of theses from the academic year 2011 in Chulalongkorn University Intellectual Repository (CUIR)
are the thesis authors' files submitted through the University Graduate School.

วิทยานิพนธ์นี้เป็นส่วนหนึ่งของการศึกษาตามหลักสูตรปริญญาวิทยาศาสตรมหาบัณฑิต
สาขาวิชาวิทยาศาสตร์พอลิเมอร์ประยุกต์และเทคโนโลยีสิ่งทอ ภาควิชาวัสดุศาสตร์
คณะวิทยาศาสตร์ จุฬาลงกรณ์มหาวิทยาลัย
ปีการศึกษา 2558
ลิขสิทธิ์ของจุฬาลงกรณ์มหาวิทยาลัย

ALL-CELLULOSE NANOCOMPOSITES FILM FROM SISAL FIBER

Mr. Noppon Somsesta

A Thesis Submitted in Partial Fulfillment of the Requirements
for the Degree of Master of Science Program in Applied Polymer Science and Textile Technology
Department of Materials Science
Faculty of Science
Chulalongkorn University
Academic Year 2015

Copyright of Chulalongkorn University

Thesis Title	ALL-CELLULOSE NANOCOMPOSITES FILM FROM SISAL FIBER
By	Mr. Noppon Somsesta
Field of Study	Applied Polymer Science and Textile Technology
Thesis Advisor	Associate Professor Duangdao Aht-ong, Ph.D.

Accepted by the Faculty of Science, Chulalongkorn University in Partial Fulfillment of the Requirements for the Master's Degree

.....Dean of the Faculty of Science
(Associate Professor Polkit Sangvanich, Ph.D.)

THESIS COMMITTEE

.....Chairman
(Assistant Professor Sireerat Charuchinda, Ph.D.)

.....Thesis Advisor
(Associate Professor Duangdao Aht-ong, Ph.D.)

.....Examiner
(Associate Professor Pranut Potiyaraj, Ph.D.)

.....Examiner
(Assistant Professor Usa Sangwatanaroj, Ph.D.)

.....External Examiner
(Tanittha Pullawan, Ph.D.)

Chulalongkorn University

นพพล สมเศรษฐ์ : นาโนคอมพอสิตฟิล์มที่เป็นเซลลูโลสทั้งหมดจากเส้นใยป่านศรนารายณ์ (ALL-CELLULOSE NANOCOMPOSITES FILM FROM SISAL FIBER) อ.ที่ปรึกษาวิทยานิพนธ์หลัก: รศ. ดร. ดวงดาว อาจองค์, 68 หน้า.

ในการศึกษาวิจัยนี้นาโนคอมพอสิตฟิล์มที่เป็นเซลลูโลสทั้งหมดได้เตรียมขึ้นโดยการใช้เซลลูโลสและเส้นใยนาโนเซลลูโลสจากเส้นใยป่านศรนารายณ์เป็นเมทริกซ์และส่วนเสริมแรงตามลำดับ เส้นใยนาโนเซลลูโลสผลิตได้โดยการใช้เตตระเมทิลพิเพอริดีน1-ออกซิล (TEMPO)/ โซเดียมไฮโปคลอไรต์/ โซเดียมคลอไรต์ในการออกซิไดซ์เซลลูโลส จากนั้นเซลลูโลสที่ผ่านการออกซิไดซ์จะถูกนำไปแยกให้เป็นเส้นใยนาโนเซลลูโลสด้วยการให้แรงเชิงกลในน้ำ ในการศึกษาลักษณะสัณฐานวิทยาของเส้นใยนาโนเซลลูโลสทำการตรวจสอบโดยการใช้กล้องจุลทรรศน์อิเล็กตรอนแบบส่องกราด ซึ่งแสดงให้เห็นถึงเส้นใยขนาดนาโนเมตรที่มีเส้นผ่านศูนย์กลางอยู่ในช่วง 10-20 นาโนเมตรและมีความยาวอย่างน้อย 1 ไมโครเมตร โดยเส้นใยนาโนเซลลูโลสเหล่านี้ถูกนำไปใส่ในสารละลายเซลลูโลสที่เตรียมได้จากการละลายเส้นใยป่านศรนารายณ์ในสารละลายลิเทียมคลอไรด์/ ไดเมทิลแอเซตาไมด์ และทำการศึกษาผลของปริมาณสารเสริมแรงที่มีผลต่อสมบัติทางสัณฐานวิทยา สมบัติทางความร้อน สมบัติทางกายภาพ และสมบัติเชิงกลของนาโนคอมพอสิตฟิล์มที่เป็นเซลลูโลสทั้งหมด ปริมาณผลึกของนาโนคอมพอสิตฟิล์มมีค่าเพิ่มขึ้นตามปริมาณของเส้นใยนาโนเซลลูโลสที่เติมลงไป ถึงแม้ว่าความทนทานต่อแรงดึงของคอมพอสิตที่มีการเติมส่วนเสริมแรง 0.5% จะลดลงจาก 40 เป็น 29 เมกะปาสคาลแต่มีการเพิ่มขึ้นอย่างมากมายของความยืดสูงสุด ณ จุดขาดจาก 11 เป็น 37% จึงกล่าวได้ว่านาโนคอมพอสิตฟิล์มมีความเหนียวทนทานมากกว่าฟิล์มเซลลูโลสที่ไม่มีการใส่สารเสริมแรง ยิ่งไปกว่านั้นเส้นใยนาโนเซลลูโลสยังช่วยเพิ่มเสถียรภาพทางความร้อนของนาโนคอมพอสิตฟิล์มได้อีกด้วย ซึ่งเห็นได้จากการเพิ่มขึ้นของอุณหภูมิเริ่มต้นของการสลายตัว สมบัติความชอบน้ำของนาโนคอมพอสิตฟิล์มลดลงเมื่อปริมาณของเส้นใยนาโนเซลลูโลสมากขึ้น โดยที่การดูดซึมน้ำจะลดลงจาก 202%เป็น 150% เมื่อมีการเติมเส้นโยนาโนเซลลูโลสลงไป 2%

ภาควิชา วัสดุศาสตร์ ลายมือชื่อนิสิต .....

สาขาวิชา วิทยาศาสตร์พอลิเมอร์ประยุกต์และเทคโนโลยีสิ่งทอ ลายมือชื่อ อ.ที่ปรึกษาหลัก .....

ปีการศึกษา 2558

5671993823 : MAJOR APPLIED POLYMER SCIENCE AND TEXTILE TECHNOLOGY
KEYWORDS: ALL-CELLULOSE NANOCOMPOSITES / CELLULOSE NANOFIBER / SISAL FIBER

NOPPON SOMSESTA: ALL-CELLULOSE NANOCOMPOSITES FILM FROM SISAL FIBER. ADVISOR: ASSOC. PROF. DUANGDAO AHT-ONG, Ph.D., 68 pp.

In this work, self-reinforced cellulose nanocomposite films were produced using cellulose and nanofiber from sisal fiber as matrix and reinforcement, respectively. Cellulose nanofiber was prepared via catalytic oxidation using TEMPO/ NaClO/ $NaClO_2$ system. By mild mechanical treatment in water, oxidized celluloses could be disintegrated into individual cellulose nanofiber and utilized as nanofiller. A morphology of TEMPO-oxidized cellulose nanofiber was characterized through transmission electron microscopy (TEM), which revealed nanosized fibrils with diameters in the range of 10–20 nm and at least 1 μm in length. These cellulosic nanofibers were subsequently impregnated in dissolved cellulose matrix which was prepared by dissolving sisal fiber in lithium chloride/N,N-dimethylacetamide solvent. The effects of reinforcement content in all-cellulose nanocomposite films were examined in terms of morphology, mechanical properties, physical properties, and thermal properties. The crystallinity of the nanocomposite films was increased as the cellulose nanofiber content went up. Even though tensile strength of 0.5% composite film was reduced from 40 to 29 MPa, elongation at break was greatly increased from 11% to 37%. These results mean that the nanocomposite films were tougher than the neat cellulose film. In addition, the cellulose nanofiber led to an improvement in the thermal stability of the nanocomposite films, as evidenced by an increment of the onset of the degradation temperature. The hydrophilicity of the nanocomposite film was decreased with an increasing amount of cellulose nanofiber. The % water absorption of the nanocomposite film was reduced from 202% to 150% with the addition of 2% nanofiber.

Department: Materials Science Student's Signature .....
Field of Study: Applied Polymer Science and Textile Technology Advisor's Signature .....
Academic Year: 2015

ACKNOWLEDGEMENTS

This thesis can not be completely finished without helping, advising, and encouraging from many people. I deeply appreciate all of the people involving in my work. It is very pleasant to work together.

First of all, I would like to express my gratitude to my thesis advisor, Associate Professor Dr. Duangdao Aht-ong for her scientific advice throughout this research. Besides the knowledge, her guidance for handling life is a precious thing for me. Together with her supports, this work can be proceeding well even though there are so many problems.

I would also like to thank the faculty and staff in Department of Materials Science, Faculty of Science, Chulalongkorn University for their supports and suggestions, especially thesis committee for their great advice and assistance: Associate Professor Dr. Pranut Potiyaraj, Assistant Professor Dr. Sireerat Charuchinda, Assistant Professor Dr. Usa Sangwatanaroj, and Dr. Tanittha Pullawan.

All my friends and co-workers are acknowledged for their contributions, helps, and scientific discussions. I thoroughly enjoy working with you, and hope we can work together in the future.

The Science Achievement Scholarship of Thailand is thanked for providing the financial support for my tuition fee and living expense throughout my study.

Finally, I would like to thank my family for their supports and encouragements.

จุฬาลงกรณ์มหาวิทยาลัย
Chulalongkorn University

CONTENTS

Page

จุฬาลงกรณ์มหาวิทยาลัย
Chulalongkorn University

Page

Page

จุฬาลงกรณ์มหาวิทยาลัย
Chulalongkorn University

LIST OF TABLES

Page

จุฬาลงกรณ์มหาวิทยาลัย
Chulalongkorn University

LIST OF FIGURES

Page

จุฬาลงกรณ์มหาวิทยาลัย
Chulalongkorn University

Page

จุฬาลงกรณ์มหาวิทยาลัย
Chulalongkorn University

CHAPTER I
INTRODUCTION

Nowadays, a plastic consumption rate is rapidly increased due to its advantages like low weight, low price, and transparent. However, plastics are a non-degradable material. This causes an accumulation of plastic wastes, and leading to one of the most serious environmental problem. To overcome this issue, cellulosic-based plastics were proposed as an alternative owning to its biodegradability.

Cellulose, one of the most abundant renewable resources, is a straight chain biodegradable homo-polymer of β-(1, 4) d-glucose units linked together in a repeating, overlapping pattern, resulting in a high tensile strength polymer. It is the main structural component of primary cell wall of plant [1]. In addition, weight of cellulosic fibers is light, owing to their low density [2].

In recent years, nanocellulose as reinforcement is a hot research area because of its extremely high surface areas. Besides biodegradability and renewability, the production of cellulosic nanofiber adds promising properties such as high mechanical characteristics and low thermal expansion [3]. However, it has been difficult to isolate cellulosic nanofiber due to the numerous of intermolecular forces (hydrogen bonding). There are many procedures to prepare nanocellulose, but the most widely used methods are mechanical and chemical processes. The chemical treatment or acid hydrolysis is applied to cellulose and the productions are generally called cellulose nanocrystals (CNCs). These rod-liked nanoparticles are also known as cellulose whiskers. The size of CNCs is around 4.7 nm wide and 143 nm long [4]. The mechanical treatment is a process in which shearing action was applied to cellulose. The separated cellulosic fibers are usually called microfibrillated celluloses (MFCs). The width is generally in the range of 3–100 nm depending on the source of cellulose, defibrillation process, and pretreatment and the length is considered to be higher than 1 μm [5]. Nevertheless, the energy consumption of this operation is too high. So, various pretreatments have been studied to solve this

problem; for example, chemical pretreatment [6], enzymatic pretreatment [7], or 2,2,6,6-tetramethylpiperidine-1-oxyl (TEMPO)-mediated oxidation [8].

Catalytic oxidation using 2,2,6,6-tetramethylpiperidine-1-oxyl (TEMPO) was utilized to cellulose for regioselective conversion of the primary hydroxyl groups to carboxylate groups. Since high density of carboxylate groups uniformly introduced on the nanofibril surfaces possess anionic charges in water, the repulsive forces occurred between the cellulose nanofibrils in water can aid separation. By mild mechanical treatment in water, oxidized celluloses can be disintegrated into individual cellulose nanofibrils.

The development of biocomposite materials by using cellulose as reinforcement still had some problems. Due to hydrophilic characteristic of cellulose, the incompatibility between cellulose and hydrophobic polymer matrix occurs, leading to low interfacial bonding. This causes an inefficient stress transfer under load and thus low mechanical strength and stiffness. Thus, the newly developed all-cellulose composites (ACCs) represent an approach to formulating green composites that aim to eliminate the chemical incompatibilities between reinforcement and matrix phases by utilizing cellulose for both components [9]. Nishino et al., who first used the concept of an all-cellulose composite, prepared cellulose solution (matrix) by dissolving pretreated ramie pulp in lithium chloride/N,N-dimethylacetamide and then impregnated the aligned ramie fiber into cellulose solution. These biocomposites showed a great potential as being a biodegradable material with good mechanical characteristic. The tensile strength of all-cellulose reinforced composite was 480 MPa, which was comparable or even higher than those of conventional glass-fiber-reinforced composites [10].

In Thailand, many agricultural wastes have been utilized as reinforcement in biocomposite films. Our previous work by Aht-ong and Somsub [11] reported the investigation of self-reinforced biodegradable cellulosic film from sisal microcrystalline cellulose (MCC) by solvent casting using NaOH/urea/thiourea aqueous solution and studied the effect of MCC content [i.e. 0, 5, 10, 15, and 20 wt%] on the properties of the composite films. The tensile strength of sisal cellulose

composite film with 15 wt% sisal MCC was 5.16 MPa. However, an addition of sisal MCC more than 15 wt% exhibited a slight decrease in tensile strength. This is because MCC can easily aggregate when the concentration of MCC was high, and could be due to the low compatibility between matrix and reinforcement. Thus, to increase the compatibility and lower an aggregation of biocomposite, this work aimed to use a nano-reinforcement filler instead of micro-scale fillers. All-cellulose nanocomposite was produced using cellulose and nanofiber from sisal fiber as matrix and reinforcement, respectively. Cellulose nanofibers were prepared via catalytic oxidation using TEMPO/ NaClO/ NaClO2 system. By mild mechanical treatment in water, oxidized celluloses can be disintegrated into individual cellulose nanofiber and utilized as nanofiller. These cellulosic nanofibers were subsequently impregnated in dissolved cellulose matrix which was prepared by dissolving sisal fiber in lithium chloride/N,N-dimethylacetamide solvent. The effects of reinforcement content in all-cellulose nanocomposite films were examined in terms of mechanical properties, physical properties, and thermal properties.

จุฬาลงกรณ์มหาวิทยาลัย
Chulalongkorn University

CHAPTER II
LITERATURE SURVEY

2.1 Cellulose

Cellulose is one of the most available and renewable biopolymers on earth, commonly exists in living organisms like animals, plants, and bacteria [3]. It has been extensively used in many industries at present. Apart from wood and cotton, cellulose can be found in the plant fibers. It is the main component of cell wall, combined with hemicellulose and lignin. Cellulose is arisen from linear D-glucose units joined through β(1–4) glycosidic bonds. The repeating units consist of two glucoses as shown in **Fig 2.1**. The degree of polymerization (DP) is in the range of 100-20000, relying on the cellulose sources [12]. Cellulose is considered to be a high mechanical properties polymer due to its highly ordered chains (crystalline structure). There are three hydroxyl groups, located at C2 and C3 (secondary hydroxyl groups) and C6 (primary hydroxyl groups). These OH groups can form intra- and intermolecular forces (hydrogen bonding) within cellulose structure, result in higher-order networks.

จุฬาลงกรณ์มหาวิทยาลัย
Chulalongkorn University

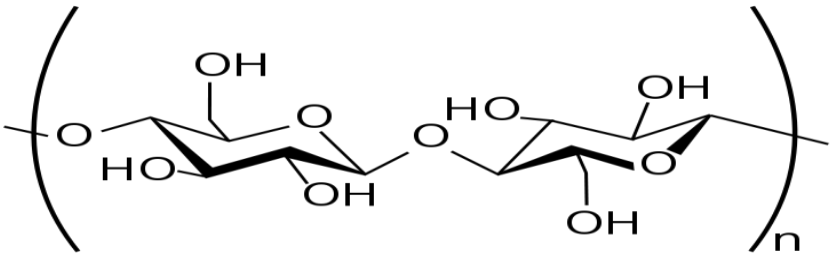

Figure 2.1 The repeating unit of cellulose.

Cellulose crystalline can be divided into four polymorphs: cellulose I, II, III, and IV (**Fig 2.2**). Cellulose I (native cellulose) occurs in two different allomorphs called as cellulose I_α and I_β. Cellulose I_α possesses a single chain triclinic structure

whereas cellulose Iβ possesses two chain monoclinic structures [13]. Both cellulose Iα and Iβ coexist in different proportions, depending on the source of the cellulose. Cellulose II is generated from cellulose I by mercerization using sodium hydroxide, or regeneration using specific solvent (e.g. N-methylmorpholine-N-oxide). In addition, there is a distinction between cellulose I and II that cellulose II composes of antiparallel chains, while cellulose I composes of parallel arrangement. Cellulose III is produced by treating cellulose I and II with ammonia. Finally, cellulose IV is obtained by heating cellulose III [14].

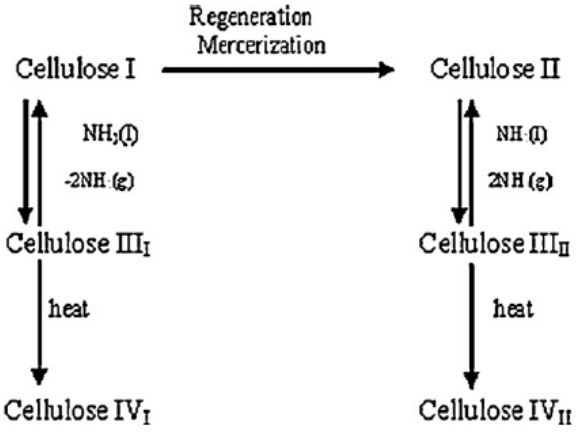

Figure 2.2 Interconversion of the polymorphs of cellulose [15].

Besides the great mechanical properties and biodegradation, cellulose is a low density material, so weight of cellulose products is light [2]. However, the existence of several hydrogen bonds causes chain stiffness and insoluble in common solvent. In fact, many industrial applications usually relate to dissolution of cellulose. A challenging issue is to deal with the structural characteristics of cellulose like biopolymeric network, the semi-crystalline structure, and numerous hydrogen bonds among molecules.

Nowadays, nanocellulose has attracted much attention due to an increasing of environmental concern, especially for using as the reinforcement or filler. Nevertheless, extraction of nanocellulose from natural resources is not easy. There is difference in chemical composition and structure formation in cellulose, depending on the sources. Moreover, various procedures (e.g., acid hydrolysis, homogenization,

sonication) are not good enough because they involve hazardous chemicals and high energy consumption [1]. A plenty of researches and studies have been proposed in order to overcome these problems, and to develop the efficient processes for isolation of nanocellulose from nature.

2.2 Nanocellulose

The term “nanotechnology” generally refers to the technology that employs of materials measuring less than 100 nm in at least one dimension. In the past few years, nanotechnology has obtained much attention, and one of the most interested research area is nanocellulose as reinforcement owing to its extremely high surface areas. Besides biodegradability and renewability, the production of nanocellulose enhances promising properties such as high mechanical characteristics with low weight and low thermal expansion [3].

Fig 2.3 shows a hierarchical structure of cellulose from plant, there are about 36 individual cellulose molecules that assemble into larger scales called as elementary fibrils or microfibrils. The diameter of elementary fibril is about 5 nm. Each of these microfibrils contains highly ordered cellulose chain (crystalline), linked along the microfibril axis by amorphous region. Then, they are wrapped up into larger scales known as microfibrillated cellulose. This microfibrillated cellulose has diameter ranging from 20 to 50 nm and several micrometers in length. Later, microfibrillated celluloses aggregate further into cellulosic fibers, along with hemicelluloses and lignin to form the plant cell wall [14].

จุฬาลงกรณ์มหาวิทยาลัย
CHULALONGKORN UNIVERSITY

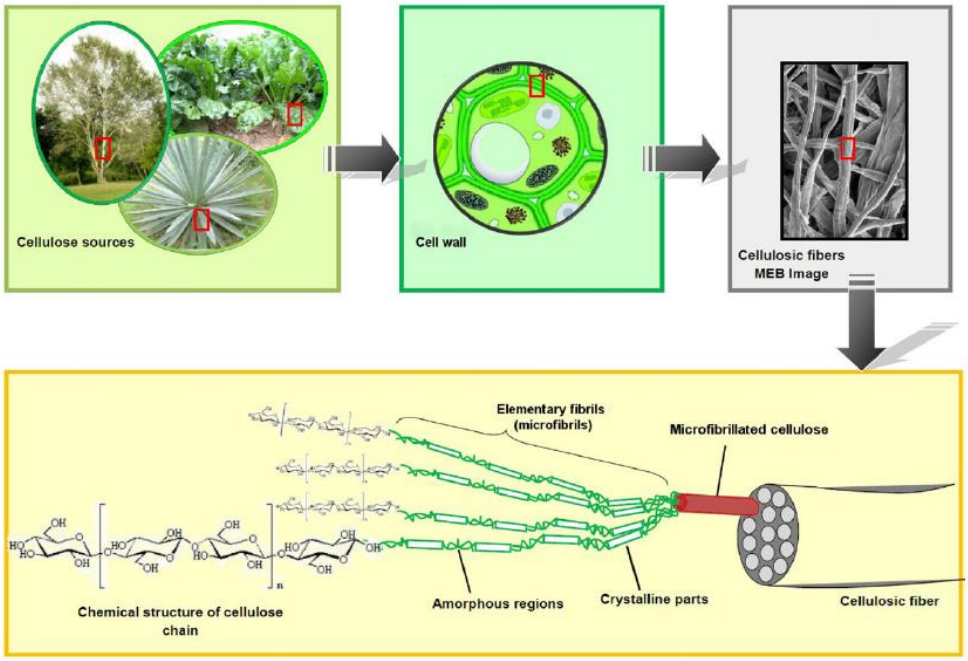

Figure 2.3 Hierarchical structure of cellulose [14].

However, it has been difficult to isolate cellulose into nano scale due to the numerous of intermolecular forces (hydrogen bonding). There are many different procedures to prepare and extract nanocellulose. All of these methods can be summarized as chemical and mechanical processes [13].

จุฬาลงกรณ์มหาวิทยาลัย
Chulalongkorn University

2.2.1 Chemical treatment

The chemical treatment is usually refered to the utilization of acid hydrolysis process for extracting nanocellulose. By controlling the strong acid, this process can efficiently remove amorphous regions and then the microfibril is separated in longitudinal axis [16]. **Fig 2.4** displays the acid hydrolysis mechanism of nanocellulose extraction. Among the strong acids, sulfuric acid is the most extensively used. This sulfuric hydrolysis generates negatively charged sulfate groups on the surface of cellulose chains through an esterification process. The negatively charged groups lead to the formation of a negative electrostatic layer on the surface and thus limit the agglomeration of nanocelluses in aqueous medium [17]. The

obtained celluloses are regularly called cellulose nanocrystals (CNCs), also known as cellulose nanowhiskers, and cellulose nanorods [3]. The morphology of CNCs

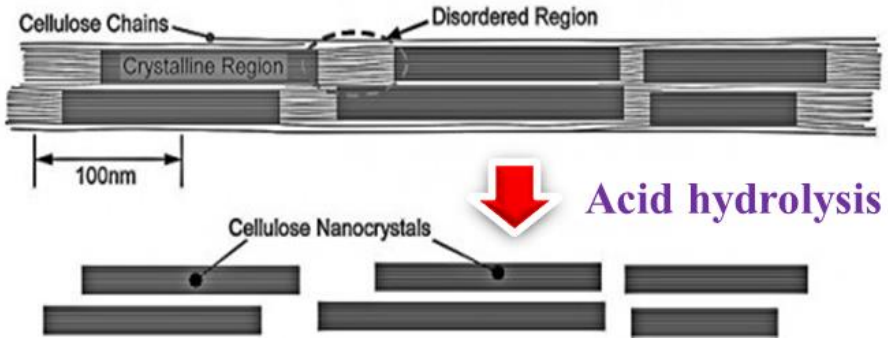

Figure 2.4 Acid hydrolysis mechanism of cellulose [18].

as showed in **Fig 2.5** revealed the rod-like nanoparticles. These nanocrystals contain highly crystalline, which varies from 54 to 88%. Generally, the length of CNCs ranges between 100 and 300 nm and the width is in range of 2 to 20 nm. The dimensions, morphology, and degree of crystallinity of CNCs rely on the source of cellulose and hydrolysis conditions [5].

Apart from acid hydrolysis, there are other processes that can isolate crystalline regions from cellulose fibers. For example; hydrolysis with gaseous acid, treatment with ionic liquids, TEMPO oxidation, and enzymatic hydrolysis treatment have been reported.

จุฬาลงกรณ์มหาวิทยาลัย
Chulalongkorn University

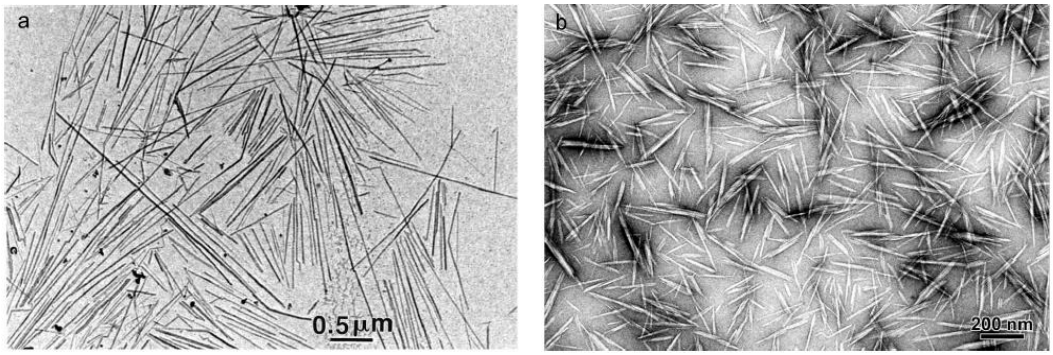

Figure 2.5 Transmission electron micrographs of cellulose nanocrystals [5].

2.2.2 Mechanical treatment

Mechanical treatment is implied to the method that an intensive mechanical force is applied to cellulosic fiber to liberating nanocellulose. Mechanical treatment can be performed in various ways: homogenization, microfluidization, grinding, cryocrushing, and high intensity ultrasonication [3]. The productions are usually called microfibrillated cellulose (MFC), also called as cellulose microfibril, microfibrillar cellulose, and nanofibrillated cellulose (NFC) [14]. **Fig 2.6** shows TEM micrographs of MFC. The MFC comprises both individual and aggregated cellulose microfibrils. This MFC is around 3-100 nm in width and at least 1 μm in length [5]. Furthermore, the degree of polymerization, morphology and aspect ratio of the MFC depend on the raw material and defibrillation methods. Unlike CNC, MFC possesses both crystalline and amorphous parts and exhibits a web-like structure. Moreover, the aspect ratio of MFC is very high, compared with CNCs [14].

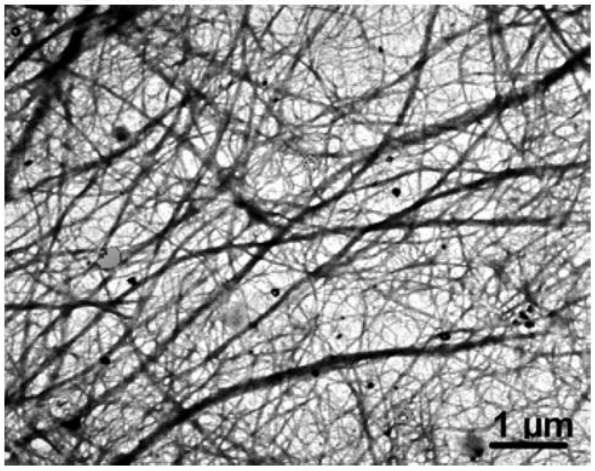

Figure 2.6 Transmission electron micrographs of microfibrillated cellulose [5].

However, high energy consumption is considered to be the major drawback for mechanical delamination process. In order to overcome this problem, various pretreatment have been offered to reduce the energy usage; for instance, enzymatic pretreatment, mechanical cutting, or 2,2,6,6-tetramethylpiperidine-1-oxyl (TEMPO)-mediated oxidation [5].

2.3 TEMPO mediated oxidation of cellulose

Catalytic oxidation using 2,2,6,6-tetramethylpiperidine-1-oxyl (TEMPO) is applied to cellulose for regioselective conversion of the primary hydroxyl groups to carboxylate groups. Owing to the presence of carboxylate groups, the anionic charges are generated when dispersing in water. Therefore, the repulsive forces occur between the cellulose nanofibrils and by mild mechanical treatment in water, oxidized celluloses can be disintegrated into individual cellulose nanofibrils. It has been published that TEMPO mediated oxidation formed only at the surface of cellulose nanofibrils and this made them still maintained their structures [19].

In the early stage, the surface modification using TEMPO/ NaBr/ NaClO was widely used as pretreatment for producing MFC. Because of high depolymerization in cellulose microfibrils, the oxidation of cellulose by TEMPO/ NaClO/ $NaClO_2$ has been proposed to avoid chain scission.

2.3.1 TEMPO/ NaBr/ NaClO

Fig 2.7 shows the oxidation mechanism of TEMPO mediated oxidation. First, NaClO oxidizes and turn NaBr into NaBrO. Then, this NaBrO converts TEMPO (a) into nitrosonium compound (b). The nitrosonium compound (b) oxidizes primary hydroxyl to carboxylate via aldehyde structure and forms N-hydroxylamine (c). Lastly, N-hydroxylamine (c) returns to nitrosonium compound (b) by TEMPO in the system.

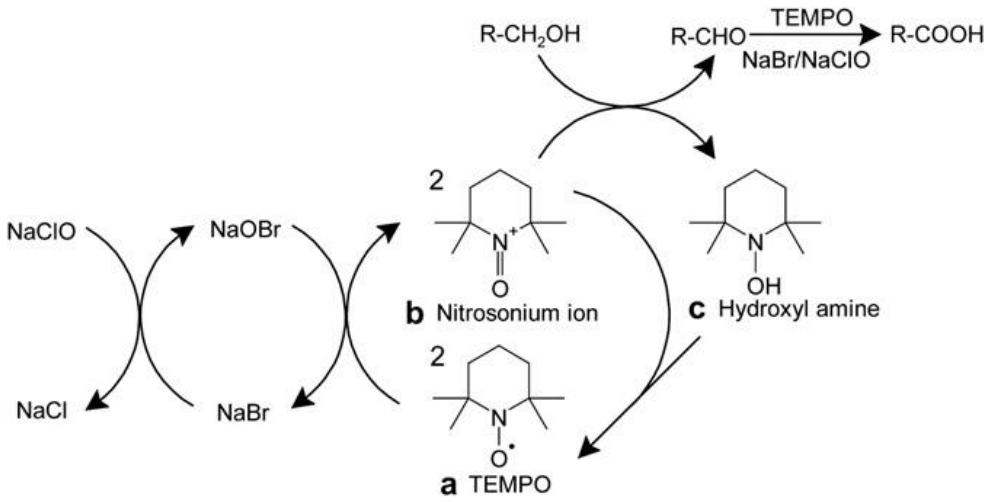

Figure 2.7 Reaction scheme of TEMPO-mediated oxidation of primary hydroxyls [20].

In 2004, Isogai and Saito [8] used 2,2,6,6-tetramethylpiperidine-1-oxyl radical (TEMPO) with sodium hypochlorite (NaClO) and catalytic amounts of sodium bromide (NaBr) to oxidize cellulose cotton linter. After the TEMPO-mediated oxidation, carboxylate and aldehyde groups formed were approximately 0.7 and 0.3 mmol/g, respectively. Crystallinities and crystal sizes of cellulose I were mostly unchanged during the oxidation, and thus, carboxylate and aldehyde groups were introduced selectively on crystal surfaces and in disordered regions. Morphology of cotton linter changed from fibrous forms to short fragments by extended oxidation time.

In 2006, Saito et al. [21, 22] oxidized bleached sulfite wood pulp and kraft pulp with TEMPO at pH 10.5. Because high density of carboxylate groups uniformly introduced on the nanofibril surfaces possess anionic charges in water, so the repulsive forces occurred between the cellulose nanofibrils in water can aid separation. By a homogenizing mechanical treatment, the TEMPO oxidized cellulose fibers were converted into transparent and highly viscous suspensions. From transmission electron microscopy results, a width of wood pulp microfibrils was around a few nanometers.

Lately, Puangsin et al. [23] also prepared individualized TEMPO-oxidized cellulose nanofibrils from hemp bast holocellulose fiber by TEMPO-mediated oxidation in water at pH 10, followed by the mechanical disintegration of

the oxidized products in water. AFM height images revealed that the nanofibril widths were 2.7–2.9 nm.

In addition, the optimum parameters for preparing cellulose nanofiber were determined by Fujisawa and coworkers [24]. They studied the effect of pH and temperature on changes in chemical structure and degree of polymerization (DP) of TEMPO-oxidized cellulose. The pH was varied from 1.0-13, while the temperature was set at room temperature through 80° C. The results showed no depolymerization occurred on oxidized cellulose in water at pH 1.0–7.0 and room temperature, while clear depolymerization took place at pH 10 and 13 by β-elimination. However, when oxidized cellulose was treated in water at pH 1.0–7.0 and temperature >50° C, the depolymerization occurred.

Okita et al. [25] applied the TEMPO-mediated oxidation to various kinds of native celluloses and measured carboxylate contents in the oxidized celluloses. The carboxylate groups varied from 0.5 to 1.7 mmol/g, depending on cellulose origins. ζ-Potentials of the oxidized cellulose microfibrils dispersed in water were approximately -75 mV for all native celluloses, although the carboxylate contents were significantly different from each other.

Shinoda et al. [26] determined degree of polymerization of wood cellulose by viscosity measurement (DPv). DPv values decreased with increasing amount of NaClO in the TEMPO-mediated oxidation stage. In addition, the association of the average lengths of TEMPO-oxidized cellulose nanofibrils (TOCNs) with their DPv values showed a linear relationship.

In 2009, Iwamota et al. [27] determined elastic modulus for single microfibrils of cellulose from Tunicate by the three-point bending test using AFM. They stated that the elastic moduli of single microfibrils prepared by TEMPO-oxidation and acid hydrolysis were 145.2 ± 31.3 and 150.7 ± 28.8 GPa, respectively.(accsub1) Later, Saito et al. estimated strengths of the single cellulose nanofibrils isolated from wood using TEMPO as a catalyst. The resulting strength ranged from 1.6 to 3 GPa [28].

For preparing cellulosic film, in 2009, Fukuzumi et al. [29] prepared films from TEMPO-oxidized cellulose nanofiber (TOCN). AFM images revealed that TOCN film surface consisted of randomly assembled cellulose nanofibers. The TOCN films were transparent and flexible and had extremely low coefficients of thermal expansion. Besbes and coworkers [30] produced cellulose nanofiber from Alfa, Eucalyptus, and Pine by TEMPO-mediated oxidation. The incorporation of nanofiber into a polymer matrix (commercial latex of poly(styrene-co-butyl acrylate), up to 15 wt% loading, imparted a high reinforcing effect to the film.

Recently, Puangsin et al. [31] oxidized three non-wood celluloses, hemp bast holocellulose, commercial bamboo, and bagasse bleached kraft pulps by TEMPO-mediated oxidation in water at pH 10 and then mechanical treatment. After disintegration, TEMPO-oxidized cellulose nanofibrils (TOCNs) were converted into self-standing TOCN films. According to AFM images, the average lengths and widths of the TOCNs were estimated to be 500–650 nm and 2.4–2.9 nm, respectively. The self-standing TOCN films had high light transparencies (>87% at 600 nm), high tensile strengths (140–230 MPa), high Young's moduli (7–11 MPa). Later, influence of TEMPO-oxidized cellulose nanofibril length on film properties was studied [32]. Various mechanical disintegration times were applied to TEMPO-oxidized cellulose nanofibrils (TOCNs) preparation. The TOCNs width was uniform ~4 nm but with three different average lengths, 200, 680, and 1100 nm. Self-standing TOCN films were prepared, shorter average TOCN lengths resulted in higher light transmittances. In contrast, a longer average TOCN length resulted in a higher tensile strength and elongation at break of TOCN films.

However, weight-average degrees of polymerization (DPw) for TEMPO-oxidized cellulose nanofibril (TOCN) prepared by TEMPO/NaBr/NaClO oxidation at pH 10 ranged from 40 to 80, which were far lower than those of the original celluloses (DPw 380–1200) used as starting materials due to the depolymerization process [33]. There are two possible ways for the depolymerization of TOCN. First, β-elimination in the case of C6 aldehyde groups formed as intermediate during oxidized under

alkaline conditions. Another one is hydroxyl radicals formed from NaBrO with TEMPO at pH 10–11 and other active species in TEMPO-mediated oxidation [34].

2.3.2 TEMPO/ NaClO/ $NaClO_2$

To overcome remarkable depolymerization, Saito et al. [35] applied TEMPO and NaClO to hardwood cellulose in water at 60° C and pH 6.8 with $NaClO_2$ used as a primary oxidant. As shown in **Fig 2.8**, NaClO oxidizes TEMPO to the N-oxoammonium ion, which then rapidly oxidizes the primary hydroxyl to aldehyde. The aldehyde is immediately oxidized to carboxyl by the primary oxidant $NaClO_2$. Hence, no aldehyde groups remain in the oxidized products, and depolymerization of cellulose chains is expected to be avoided. The oxidized celluloses were then converted to highly crystalline and individual fibrils having 5 nm in width and at least 2 μm in length by disintegration in water. The oxidized celluloses had no aldehyde groups, and had high degrees of polymerization of more than 900. The prepared films were transparent and flexible, and exhibited a high tensile strength of 312 MPa even at a low density of 1.47 g/cm^3.

จุฬาลงกรณ์มหาวิทยาลัย
Chulalongkorn University

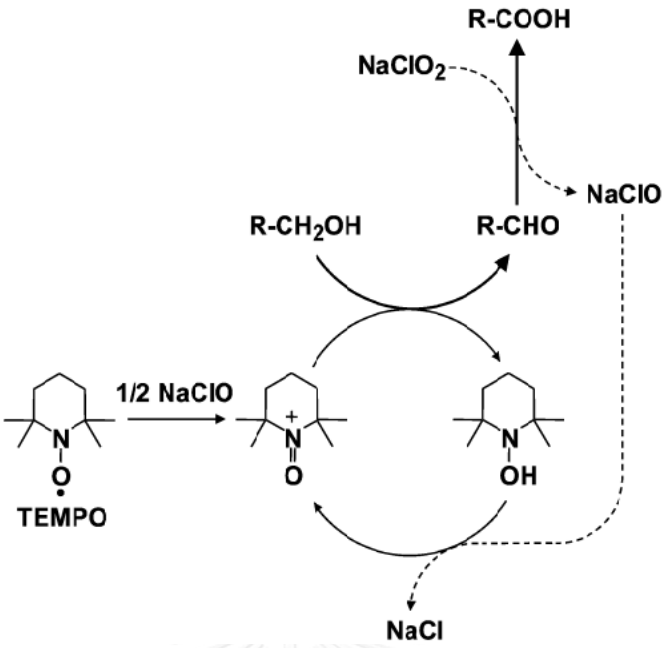

Figure 2.8 Oxidation of primary hydroxyls to carboxyls by the TEMPO/ NaClO/ $NaClO_2$ system [35].

Next year, Saito et al. [19] further investigated the effects of oxidation conditions by TEMPO/NaClO/$NaClO_2$ system on carboxylate content and degree of polymerization (DP) of bleached wood pulp. The oxidation was more accelerated by the addition of NaClO at pH 6.8 and 40– 60° C. Addition of NaClO of more than 0.5 mmol/g of the pulp was effective to accelerate the oxidation. Eventhough DP of oxidized pulp gradually decreased with reaction time, the DP values of more than 900 were maintained for all the oxidized pulps. Lately, Tanaka and coworkers [36] prepared cellulose nanofibrils from softwood cellulose by TEMPO/NaClO/$NaClO_2$ systems in water at pH 4.8 or 6.8. When the TEMPO-mediated oxidation was applied to softwood cellulose in water at pH 6.8 and 40° C, the carboxylate content rose to ~0.8 mmol/g after reaction for 24 h and the DP value was more than 1100. Then, the oxidized cellulose was converted to individual nanofibrils by mechanical disintegration in water, with uniform widths of 3–4 nm and lengths greater than 1 μm.

2.4 Sisal fiber

Sisal fiber is one of the most broadly used natural fibers. It has been produced commercially and about 4.5 million tons of sisal fibers are generated every year. Brazil and Tanzania are currently the largest producer of sisal fiber.

The sisal plant is presented in **Fig 2.9**. Sisal fiber is a very strong fiber extracted from the leaves of the sisal plant (*Agave sisalana*). Sisal plant produces 200–250 leaves. The sisal leaf has a sandwich structure and each leaf contain 1000-1200 fiber bundles which is consisted of 4% fiber, 0.75% cuticle, 8% dry matter, and 87.25% water. Thus, the dried fiber is only 4% of the total weight of the leaf [37].

Figure 2.9 Photograph of a sisal plant.

จุฬาลงกรณ์มหาวิทยาลัย
CHULALONGKORN UNIVERSITY

According to Faruk, the chemical composition of sisal fiber has been reported in **Fig 2.10**. Sisal fiber contains 65 % cellulose, 12 % hemicellulose, 9.9 % lignin, and 2% waxes. The diameter of sisal fiber is about 100-300 mm and length is in a range of 1.0-1.5 m. The main constituents of sisal fiber are cellulose, hemicellulose, and lignin. In the synthesis of plant cell wall, polysaccharides such as cellulose and hemicellulose are formed simultaneously and lignin fulfills the space between the polysaccharide to link them together. This lignification process makes a tightening of cell wall, and prevents the carbohydrate from physical and chemical damage [38].

Figure 2.10 Chemical composition of some common natural fibers [39].

Fiber	Cellulose (wt%)	Hemicellulose (wt%)	Lignin (wt%)	Waxes (wt%)
Bagasse	55.2	16.8	25.3	-
Bamboo	26–43	30	21–31	-
Flax	71	18.6–20.6	2.2	1.5
Kenaf	72	20.3	9	-
Jute	61–71	14–20	12–13	0.5
Hemp	68	15	10	0.8
Ramie	68.6–76.2	13–16	0.6–0.7	0.3
Abaca	56–63	20–25	7–9	3
Sisal	65	12	9.9	2
Coir	32–43	0.15–0.25	40–45	-
Oil palm	65	-	29	-
Pineapple	81	-	12.7	-
Curaua	73.6	9.9	7.5	-
Wheat straw	38–45	15–31	12–20	-
Rice husk	35–45	19–25	20	14–17
Rice straw	41–57	33	8–19	8–38

Ramzy and coworker [40] reported that tensile strength of sisal fiber varied from 363 to 700 MPa with the density in the range of 1.33-1.55 g/cm^3. The variability arose from the different sources of the sisal fiber and measurement methods.

Sisal fiber is a strong fiber commonly used for manufacturing rope, twine, cordage, especially in agricultural and marine industry. Due to its advantages (i.e. biodegradable, low density, high specific strength), sisal fiber has a great potential to be utilized as reinforcement. In addition, the price of sisal fiber is very low compared with synthetic fibers. This causes growing interest in manufacturing composites industries that can be used in automobiles, building materials, locomotives, and other applications which aims to replace synthetic fibers.

2.5 Composite material

A composite material is defined as a material which is composed of two or more constituent materials with significantly different physical or chemical properties and results in better features than those of the individual ingredient used solely [41]. Generally, the structure of composite material consists of a reinforcement (e.g. particles, fillers, and/or fibers) embedded in a matrix (e.g. metal, ceramic, or polymer). The matrix phase performs several function; for instance, holding the reinforcement together, keeping the reinforcement in the suitable orientation, and protecting the reinforcement from environment. Moreover, one of the main tasks of the matrix is to transfer stress into the reinforcement when external force is applied to the composite material. Another part of the constituent is reinforcement. The reinforcing phase can appear in different forms (i.e. particles, flake, and fibers). It is supposed to be the toughest part among the constituents. Thus, the major role of reinforcement is to improve mechanical properties of the composite material [42].

It can be considered that composite material is tailorable. The different properties can be obtained by properly choosing their constituent, their ratios, their orientations, their morphologies, their crystallinity, structure and composition of the interface between components. Because of this tailorability, composite materials are extensively utilized in various applications. For example, a high stength lightweight structural composite is produced by embedding carbon fibers in a matrix. The fibers provide strength and stiffness while the matrix acts as binder. Apart from lower weight, the other benefits of composite material are listed below [43].

- Tailorable properties
- Longer life (chemical and corrosion resistance)
- Low friction coefficient and good wear resistance
- Increased or decreased electrical or thermal conductivity
- Dimensional stability (can be designed for zero CTE)
- Increase strength and stiffness
- Toughness and damage tolerance (by using proper fiber orientations)

- Maintain strength/stiffness at high temperature

Although composite materials provide a lot of advantages, they still have some disadvantages. The cost of matrix and reinforcement is expensive. Moreover, some forming processes are complicated, so they require high technology instruments to manufacture. Due to their tough characteristic, it is hard to eliminate the composite materials. Some of these wastes may remain in environment and cause pollution.

2.6 Classification of composite material

According to the type of matrix used, composite materials are classified into three main classes as discussed below [44].

- **Metal-Matrix Composites (MMCs)**: A metal matrix is particularly good for high temperature use in corrosive environment. In addition, the metal composites provide high strength, stiffness, and fracture toughness. The most normally used metals are titanium, aluminum, iron, tungsten, nickel, and magnesium. At present, they are not as widely in use as PMCs due to their heavy weight. Most metal composites could be used as matrices in case they require materials which have to be stable over a range of temperature and non-reactive. In most of' the advanced countries, metal composites are gaining popularity as an alternative materials, especially in the fields of missiles, ordnance, space and electronics.
- **Ceramic-Matrix Composites (CMCs)**: A ceramic matrix possesses strength at high temperature well above 1500 $^{\circ}$ C. Besides that, they provide high melting point, low thermal expansion, high elastic modulus, and good chemical & weather resistance. Nevertheless, the major drawback of ceramics is that they are usually brittle. The ceramic matrices are usually carbides (SiC), nitrides (SiN_4, BN), and

oxides (Al_2O_3, Zr_2O_3, Cr_2O_3, Y_2O_3, CaO, ThO_2). These materials are usually utilized under the most extreme operating environment, typically used in applications such as seal rings, pump, and valves.

- **Polymer-Matrix Composites (PMCs)**: A polymer matrix is the most common and least cost. It is greatly more popular than other two matrices. Almost all kind of reinforcements can be used with polymers to provide a wide range of properties. Furthermore, it possesses lightweight, easily processable, and desirable mechanical properties. In general, there are two main kinds of polymer, namely, thermosets and thermoplastics. Thermoset is a polymer with highly cross-linked chains and after processed it can not change structure. The most generally used thermosets are epoxy, polyester and phenolic resins. Thermoset matrix is sometimes employed in high temperature condition. Thermoplastic is a polymer with non-cross-linked chain, thus it can change structure when it reaches melting temperature. The most common thermoplastic polymers are polyethylene, polyvinyl alcohol, and polycarbonates. Nowadays, polymer matrices are extensively used in various applications.

จุฬาลงกรณ์มหาวิทยาลัย
Chulalongkorn University

2.7 All-cellulose composite

Due to an increasing of environmental concern, a lot of attentions have been paid to sustainable, green, and environmentally friendly materials for a variety of applications [3]. In order to follow these aspects, biodegradable fiber reinforced composite materials have been developed. However, the development of biocomposite materials by using cellulose as reinforcement still has some problems. Due to hydrophilic characteristic of cellulose, the incompatibility between celluloses and hydrophobic polymer matrix occurs, leading to low interfacial bonding. This causes an inefficient stress transfer under load and thus low mechanical strength and stiffness. To overcome poor interfacial bonding, several methods have been purposed. The most common procedures are fiber or matrix surface modification and filling some coupling agents or compatibilizers but these processes are increasing costs and spending more times [45]. Thus, the newly developed all-cellulose composites (ACCs) represent an approach to formulating green composites that aim to eliminate the chemical incompatibilities between reinforcement and matrix phases by utilizing cellulose for both components [9].

In general, there are two main strategies to produce all-cellulose composites (**Fig 2.11**). For the first approach (2-step method), a portion of cellulose is primarily dissolved in a solvent and thus the solution regenerates in the presence of other undissolved cellulose constituent. For another method (1-step method), cellulosic fibers are partially dissolved in solvent. This dissolution of cellulose takes place on their surfaces and then regenerates in situ to form a matrix around the undissolved portion [46].

จุฬาลงกรณ์มหาวิทยาลัย
Chulalongkorn University

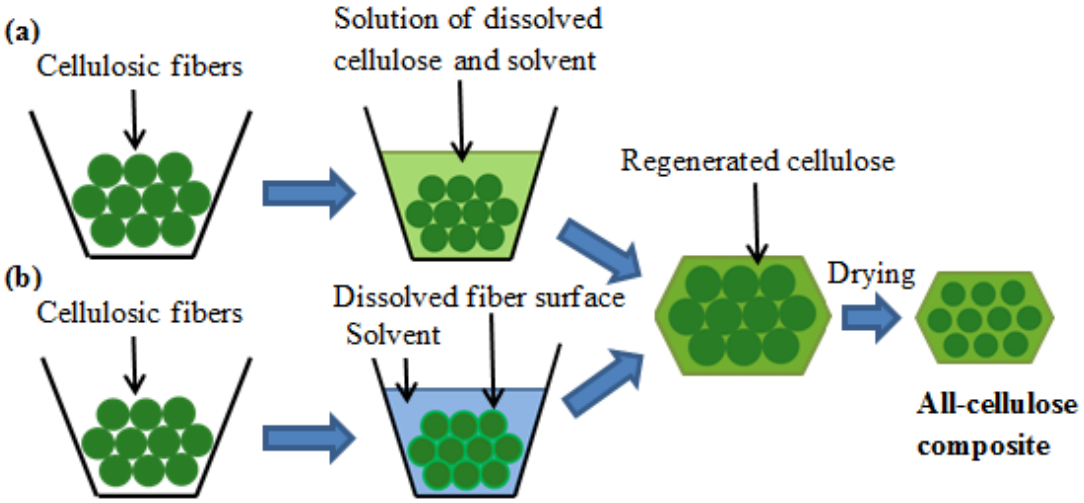

Figure 2.11 Schematic of two-step (a) and one-step (b) all-cellulose composite preparation [9].

Although various solvents can be used for dissolving cellulose, there are three common solvents that usually use for preparation of all-cellulose composites, including NaOH aqueous solution with additives, lithium chloride/N,N-dimethylacetamide (LiCl/DMAc), and ionic liquids (ILs).

For dissolution of cellulose in NaOH aqueous solution with the addition of urea, the solution needs to be done at sub-zero temperature, about -12 to -15° C. Normally, NaOH can only dissolve low DP of cellulose, the addition of urea ($(NH_2)_2CO$) and/or thiourea ($(NH_2)_2CS$) to aqueous NaOH considerably increase the solubility. When alkaline solvent reaches sub-zero temperature, the solution is regularly stirred in order to dissolve the cellulose. By centrifugation, the truly dissolved cellulose can be separated from the undissolved part. The dissolved part is subsequently converted into a gel by a thermal path or precipitated in an acidic medium or coagulant [9].

Another solvent for dissolution of cellulose is DMAc mixed with LiCl. First, cellulose has to take an activation process in order to efficiently and fully dissolve cellulose. Without this, the dissolution process may spend several months. The dissolving mechanism is supposed to go via an intermediate involving the interaction

of Cl^- with cellulose. The intermediate complexes of LiCl salts are occurred at cellulose hydroxyl group (**Fig 2.12**). Due to the presence of Cl^-, the negative charges are generated and cause molecules repulsive force. Moreover, it decreases the hydrogen bond effect between the cellulose molecules, along with stirring cellulose can be fully dissolved and further use for preparation of all-cellulose composites [12].

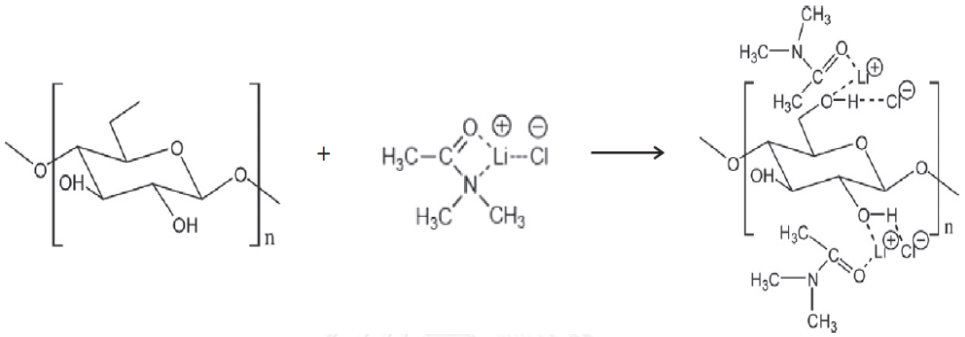

Figure 2.12 Example of a hydrogen-bond breaking mechanism for the cellulose dissolution in the lithium chloride/dimethylacetamide (LiCl/DMAc) solvent system [12].

The other common utilized solvent in all-cellulose composites preparation is ionic liquids (ILs). Ionic liquids are molten salts with melting points below 100° C. There are massive possible combinations of different cations and anions however just only some of them can be used to dissolve cellulose. The most successful mixtures are hydrophilic consisting of methylpyridinium or methylimidazoloium cation cores with ethyl-, butyl-, or allyl- side chains mixed with formate, acetate, or chloride anions. The solubility of ILs to dissolve cellulose originates from their high effective polarity, due to their ionic character.

The concept of all-cellulose composites was first discussed by Nishino and coworkers. They produced all-cellulose composites by using cellulose solution (dissolving pretreated ramie pulp in lithium chloride/N,N-dimethylacetamide) as matrix, and aligned ramie fibers as reinforcement. The all-cellulose composites exhibited a promising potential as being a biodegradable material with good

mechanical property. The tensile strength of the biocomposite was 480 MPa. It was equal or even higher, compared to those of conventional glass-fiber-reinforced composites [10]. Later, Qin et al. [47] prepared all-cellulose composites with 85–95% ramie fibre volume fraction by using cellulose solution (dissolved ligno-cellulosic ramie fibres in LiCl/DMAc) and investigated the effect of alkali treatment to the biocomposites. After treatment, tensile strength of the prepared composites was improved by 15–95%. Soykeabkaew et al. [45] fabricated all-cellulose composites by a surface selective dissolution method of aligned ligno-cellulosic fibres using lithium chloride/N,N-dimethylacetamide as a solvent. Composites with optimized immersion time showed great mechanical properties. A longitudinal tensile strength and Young's modulus were 460 MPa and 28 GPa, respectively. In 2009, Duchemin and coworkers [48] made all-cellulose composites by partly dissolving microcrystalline cellulose (MCC) powder in a 8% LiCl/DMAc solution. Cellulose solutions were precipitated and the resulting gels were dried in a vacuum bag to produce films. The precipitation conditions were found to play a major role in the optimization of the mechanical properties. All-cellulose composites were produced with a tensile strength up to 106 MPa and a tensile modulus up to 7.6 GPa. Lately, Aht-ong and Somsub [11] prepared self-reinforced biodegradable cellulosic film by solvent casting using NaOH/urea/thiourea aqueous solution and sisal microcrystalline cellulose (MCC) as matrix and reinforcement, respectively. They reported that the tensile strength of sisal cellulosic composite film with 15 wt% was 5.16 MPa. Nevertheless, an addition of sisal MCC more than 15 wt% caused a slight decrease in tensile strength. This was because MCC can easily aggregate when the concentration of MCC was high, and could be owing to the poor compatibility between matrix and reinforcement.

In order to avoid aggregation of reinforcement and increase the chemical compatibility, the nanoscale reinforcements have been utilized instead of microscale fillers. Pullawan and coworkers [49] produced all-cellulose composites using microcrystalline cellulose (MCC) solution (dissolved in a solvent of LiCl/DMAc) as the matrix and cellulose nanowhiskers (CNWs), produced by acid hydrolysis, as the reinforcement. The tensile strength values of 0.5% and 1.0% volume fractions

nanocomposites were 111.2 and 128.4 MPa, respectively. Another Pullawan's research in 2013, cellulose nanowhiskers (CNWs) were used to reinforce an all-cellulose composite. This composite comprised a matrix formed by dissolution of plant cellulose using a LiCl/DMAc solvent. They reported that mechanical properties of nanocomposites decreased greatly when the material was wetted, due to disengagement of the hydrogen bonds between the matrix and CNWs by moisture [50]. Alcala et al. [51] isolated nanofibrillated cellulose (NFC) from bleached eucalyptus pulp, and used as reinforcement in an unbleached eucalyptus fiber matrix. The 9 wt% NFC nanocomposites showed excellent properties that the tensile strength and Young's modulus improved linearly, increasing up to 150 and 60 %, respectively, compared with unreinforced film. Recently, Ghaderi and coworkers [52] produced all-cellulose nanocomposite (ACNC) film from sugarcane bagasse nanofibers using LiCl/DMAc solvent. This ACNC film possessed great mechanical properties and lower water vapor permeability, so these biocomposite films had potential for the development of protective film in food packaging industries. Similarly, Zhao et al. [53] extracted cellulose nanofibrils (CNFs) with diameters around 15–40 nm from softwood pulp via simple physical methods. Self-reinforced nanocomposite films were prepared using CNFs as fillers and LiCl/DMAc dissolved regenerated cellulose as the matrix. When the CNFs content was increased from10 wt% to 20 wt%, the tensile strength of the biocomposite films increased from 61.56 MPa to 99.92 MPa and the Young's modulus increased from 0.76 GPa to 4.16 GPa. In 2014, Pullawan et al. [54] dispersed cellulose nanowhiskers in two different matrix systems. These two matrixs were produced by lithium chloride/N,N-dimethyl acetamide (LiCl/DMAc) and sodium hydroxide/urea (NaOH/urea). They reported that mechanical properties of composites comprising a LiCl/DMAc based matrix were better than NaOH/urea based systems.

CHAPTER III
EXPERIMENTAL

3.1 Materials and Chemicals

3.1.1 Sisal fiber

- was purchased from Hubkapong Agricultural Cooperation, Phetchaburi province, Thailand.

3.1.2 Sodium hydroxide (NaOH)

- was purchased from RCI Labscan, Samutsakorn, Thailand and was used to delignify and bleach sisal fiber.

3.1.3 Hydrogen peroxide (H_2O_2)

- was purchased from QRëC, New Zealand and was used to bleach sisal fiber.

3.1.4 2,2,6,6-tetramethylpiperidine-1-oxyl radical (TEMPO)

- was purchased from Sigma-Aldrich, Hamburg, Germany and was used to oxidize bleached sisal cellulose. Its chemical structure is shown in **Fig 3.1**.

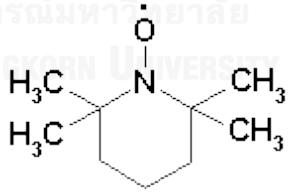

Figure 3.1 Chemical structure of TEMPO

3.1.5 Sodium hypochlorite (NaClO)

- was purchased from Ajax Finechem, Auckland, New Zealand and was used to oxidize bleached sisal cellulose.

3.1.6 Sodium chlorite ($NaClO_2$)

- was purchased from Ajax Finechem, Auckland, New Zealand and was used to oxidize bleached sisal cellulose.

3.1.7 Sodium phosphate monobasic dihydrate ($NaH_2PO_4.2H_2O$)

- was purchased from Ajax Finechem, Auckland, New Zealand and was used as buffer during oxidation of bleached sisal cellulose.

3.1.8 Sodium phosphate dibasic heptahydrate ($Na_2HPO_4.7H_2O$)

- was purchased from Panreac, Barcelona, Spain and was used as buffer during oxidation of bleached sisal cellulose.

3.1.9 Lithium chloride (LiCl)

- was purchased from Ajax Finechem, Auckland, New Zealand and was used to dissolve bleached sisal cellulose.

3.1.10 N,N-dimethylacetamide (DMAc)

- was purchased from RCI Labscan, Samutsakorn, Thailand and was used to dissolve bleached sisal cellulose. Its chemical structure is shown in **Fig 3.2**.

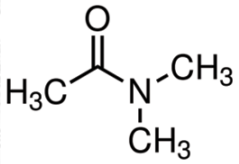

Figure 3.2 Chemical structure of DMAc

จุฬาลงกรณ์มหาวิทยาลัย
Chulalongkorn University

3.1.11 Acetone

- was purchased from RCI Labscan, Samutsakorn, Thailand and was used to dehydrate water from activated bleached sisal cellulose.

3.2 Equipment and instruments

The equipment and instruments utilized in this research were listed in Table 3.1 and 3.2.

Table 3.1 Equipment and instruments used in preparation of all-cellulose nanocomposite films

Equipment and instruments	Model	Company/City/Country
Hotplate stirrer	C-MAG HS 7	IKA, Wilmington, North Carolina
Homogenizer (**Fig 3.3**)	T18 Ultra Turrax	IKA, Wilmington, North Carolina
Ultrasonic homogenizer (**Fig 3.4**)	Vibra cell	SONICS, Newtown, Connecticut
Sonicator bath (**Fig 3.5**)	TRU-SWEEP	Crest Ultrasonics, Penang, Malaysia
Disk mill (**Fig 3.6**)	PULVERISETTE	FRITSCH, Idar-Oberstein, Germany

Figure 3.3 T18 Ultra Turrax, IKA Homogenizer

Figure 3.4 Vibra cell, SONICS Ultrasonic homogenizer

Figure 3.5 TRU-SWEEP, Crest Ultrasonics Sonicator bath

Figure 3.6 PULVERISETTE, FRITSCH Disk mill

Table 3.2 Equipment and instruments employed in characterization and testing

Equipment and instruments	Model	Company/City/Country
Zeta potential analyzer	ZetaPALS	Brookhaven, Holtsville, New York
Fourier transform infrared spectroscopy (FT-IR)	Nicolet 6700	Thermo Fisher Scientific, Waltham, Massachusetts
Transmission electron microscope (TEM)	Tecnai 20 Twin	FEI Company, Hillsboro, Oregon
Thermogravimetric Analyzer (TGA)	TGA/SDTA 851[e]	Metter Toledo, Columbus, Ohio
Universal testing machine	LLOYD LR 100K	LLOYD INSTRUMENTS, West Sussex, England
Scanning electron microscope (SEM)	JSM 6400	JEOL, Tokyo, Japan
X-ray diffractometer (XRD)	Bruker AXS Diffraktometer D8	Bruker, Karisruhe, Germany

จุฬาลงกรณ์มหาวิทยาลัย
Chulalongkorn University

3.3 Experimental Procedure

3.3.1 Sisal cellulose extraction

The dried sisal fiber was cut into small pieces having 2 mm in length. Delignification of sisal fiber was performed with 2 M NaOH at 60° C for 4 hr. This process was adapted from Somsub [11]. The delignified fiber was subsequently bleached by 10% H_2O_2 in 10 % NaOH at 70° C for 70 min, two times. Afterthat, the bleached fiber was washed with distilled water, and then dried in hot air oven at 60° C. The obtained fiber was ground, and further used as precursor for preparing cellulose solution and cellulose nanofiber.

3.3.2 TEMPO-mediated oxidation of sisal fiber

The bleached sisal cellulose (1g) was suspended in 0.1 M sodium phosphate buffer (100 ml, pH 6.8), containing TEMPO (0.1 mmol) and sodium chlorite

(10 mmol) in an airtight flask. A 2 M sodium hypochlorite solution (2 ml, 4 mmol) was added to the flask, and immediately stoppered. The slurry was strirred at 60° C for 18 h. The oxidized cellulose was washed with water by filtration using filter paper no.4, and dried in hot air oven at 60° C.

3.3.3 Preparation of cellulose nanofiber

The tempo-oxidized cellulose suspended in water (50ml) at a 0.1 % (w/v) solid content was homogenized for 4 min at 7500 rpm with a homogenizer (T18 Ultra Turrax, IKA, Wilmington, North Carolina), and then sonicated for 10 min using an ultrasonic homogenizer equipped with a 7 mm probe tip (Vibra cell, SONICS, Newtown, Connecticut) at 20 kHz. The slurry was dried in hot air oven at 80° C. Then, the obtained cellulose nanofiber was kept in a dessicator at an ambient condition for further used as reinforcement fiber.

3.3.4 Preparation of cellulose solution

The bleached sisal cellulose (2g) was activated for 5 h in water at room temperature to swell the material. Next, this swollen material was dehydrated in acetone and dimethylacetamide (DMAc) for 5 h and 4 h, respectively. Meanwhile, a solvent solution of 8 wt% LiCl in DMAc was prepared and stirred at 60° C for 60 min. The activated cellulose was dissolved in LiCl/DMAc solution by magnetic stirring at room temperature for a week.

จุฬาลงกรณ์มหาวิทยาลัย
Chulalongkorn University

3.3.5 Preparation of All-cellulose nanocomposites films

A desired amount of cellulose nanofiber was suspended in DMAc and sonicated for 6 h. The suspension was subsequently mixed with cellulose solution and stirred vigorously to form a homogeneous mixture. The resultant mixture was poured into a glass plate and kept at ambient condition for 8 h to form a gel. A gel film was washed with water, and then air dried at ambient temperature. The films containing (0, 0.5, 1, and 2% w/v) reinforcement were defined as SC0, SC0.5, SC1, and SC2, respectively.

The overall of experimental procedure performed in this research, including the characterization and testing of all-cellulose nanocomposite film, was displayed in **Fig 3.7**.

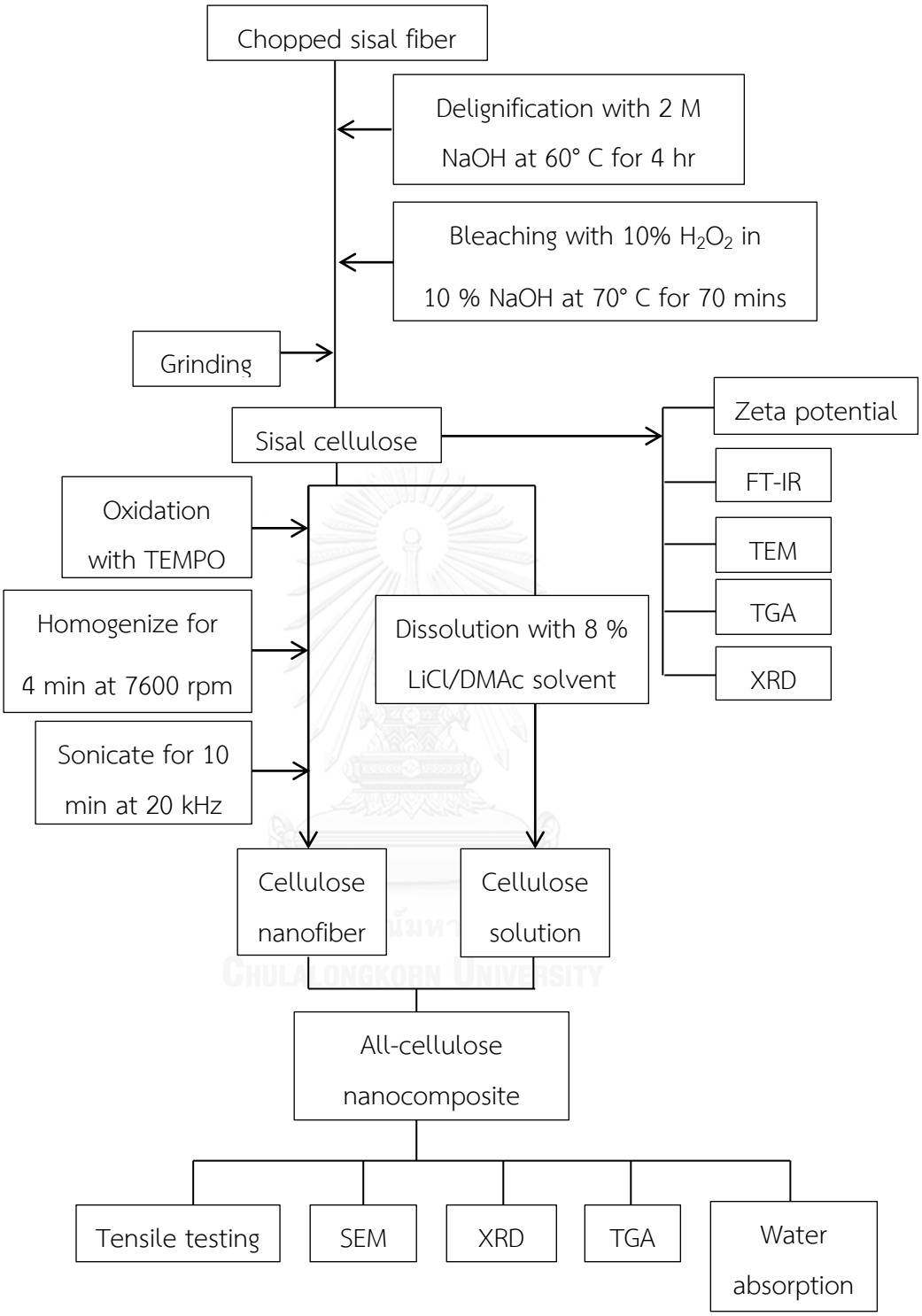

Figure 3.7 Flow diagram of the experimental method

3.4 Characterization and Testing

3.4.1 Characterization of cellulose nanofiber

3.4.1.1 Zeta potential measurement

A measurement of zeta potential was used to estimate the surface charges of colloidal particle. The zeta potential of oxidized cellulose nanofiber dispersed in water at a consistency of 0.1% (w/v) was measured at 25 ° C using a zeta potential analyzer (ZetaPALS, Brookhaven, Holtsville, New York) as shown in **Fig 3.8**.

Figure 3.8 ZetaPALS, Brookhaven Zeta potential analyzer

3.4.1.2 Morphological studies

The cellulose nanofiber suspension (0.1% w/v) was mounted on a glow-discharged carbon-coated Cu grid. The excess liquid was absorbed by a filter paper, and one drop of 1% uranyl acetate was added for negative staining of the cellulose nanofiber, then blotted with filter paper to remove excess solution and allowed to dry under the ambient condition. The sample was observed with transmission electron microscope (TEM) (Tecnai 20 Twin, FEI Company, Hillsboro, Oregon). The diameter and length of cellulose nanofiber was measured and calculated using ImageJ software.

3.4.1.3 FT-IR spectroscopy

The functional group of oxidized cellulose was determined using fourier transform infrared spectroscopy (Nicolet 6700, Thermo Fisher Scientific, Waltham, Massachusetts) as shown in **Fig 3.9**. The spectra were recorded at 4 cm^{-1} resolution, in the range between 400 and 4000 cm^{-1}. The samples were ground, and then blended with KBr followed by pressing into pellets.

Figure 3.9 Nicolet 6700, Thermo Fisher Scientific FTIR spectrometer

3.4.1.4 Thermogravimetric Analysis

Thermal decomposition temperatures were examined under a nitrogen atmosphere using a thermogravimetric analyzer (TGA/SDTA 851^{e}, Metter Toledo, Columbus, Ohio) as shown in **Fig 3.10**. A 10 mg of cellulose nanofiber was tested in a temperature range between 30 and 600 ° C at a heating rate of 10° C/min.

Figure 3.10 TGA/SDTA 851^{e}, Metter Toledo Thermogravimetric analyzer

3.4.1.5 X-ray diffraction

The crystallinity of cellulose nanofiber was characterized by X-ray diffractometer (Bruker AXS Diffraktometer D8, Bruker, Karisruhe, Germany) as shown in **Fig 3.11** with Cu Kα radiation (λ=0.1540 nm) at 40 kV and 40 mA. Diffractograms were collected in the range of 2θ = 5-40 ° at a scanning rate of 2 ° min^{-1}. The crystallinity of cellulose nanofiber was calculated by the empirical Segal's equation [55]:

$$\chi = [(I_{200} - I_{am})/I_{200}] \times 100 \qquad \textbf{Eq. 1}$$

where I_{200} is the diffraction intensity of the (2 0 0) lattice reflection, which is located at 2θ = 22°. I_{am} is the intensity recorded at 2θ = 18°; the area of maximum intensity for fully amorphous cellulose.

Figure 3.11 Bruker AXS Diffraktometer D8, Bruker, Karisruhe X-ray diffractometer

3.4.2 Characterization of all-cellulose nanocomposite films

3.4.2.1 Physical properties

3.4.2.1.1 Morphological studies

Morphological analysis of the composite films was investigated by scanning electron microscope; SEM (JSM 6400, JEOL, Tokyo, Japan) at 10 kV accelerating voltage. The fracture surface of all-cellulose nanocomposite films was coated with gold using sputtering technique and subsequently observed.

3.4.2.1.2 Crystallinity

X-ray diffraction profiles of the composite films were recorded by X-ray diffractometer (Bruker AXS Diffraktometer D8, Bruker, Karisruhe, Germany) as shown in **Fig 3.11** with Cu Kα radiation (λ=0.1540 nm) at 40 kV and 40 mA. The XRD curves were collected in the range of 2θ = 5-40 ° at a scanning rate of 2 ° min^{-1}. The cellulose crystallinity was determined using Segal's equation (**Eq.1**).

3.4.2.1.3 Water absorption

Water absorption of all-cellulose nanocomposite films was measured according to ASTM D 570 standard. All specimens were dried in an oven at 60° C (for 24 h prior to testing), and immediately weighed (W_1). The specimens were then placed in container of water and maintained at ambient condition. After specific period of time (4, 8, 12, and 24h), the specimens were removed from the water. All surfaces were then wiped with dry cloth, and weighed suddenly (W_2). Percentage increase in weight during immersion was calculated as follows:

$$\% \text{ Water absorption} = [(W_2 - W_1)/W_1] \times 100 \qquad \textbf{Eq. 2}$$

3.4.2.2 Mechanical properties

Mechanical testing of composite films was performed using a universal testing machine (LLOYD LR 100K, LLOYD INSTRUMENTS, West Sussex, England) as shown in **Fig 3.12** at a speed of 5 mm/min. The specimens of 5 mm in width and 50 mm in length were cut off from the composite films. Eight specimens were tested for each sample, and the average values were calculated and reported together with standard deviation.

Figure 3.12 LLOYD LR 100K, LLOYD INSTRUMENTS universal testing machine

จุฬาลงกรณ์มหาวิทยาลัย
Chulalongkorn University

3.4.2.3 Thermal properties

Thermal degradation behaviour of the composite films was assessed by thermogravimetric analyzer (TGA/SDTA 851^{e}, Metter Toledo, Columbus, Ohio) as shown in **Fig 3.10**. Specimen weight approximately 10 mg was examined in temperature range of 30-600° C at a heating rate of 10° C/min under nitrogen atmosphere.

Chapter IV
RESULTS AND DISCUSSION

4.1 Characterization of cellulose nanofiber

First of all, the proper condition for preparing cellulose nanofiber was studied and the results were shown in **Table 4.1**. In oxidation process, the effects of the amount of the oxidizing agent and the oxidation time on the oxidation efficiency were examined. Different amounts of sodium hypochlorite 2, 4, and 6 mmol were applied to cellulose. The results revealed that 2 mmol sodium hypochlorite had low efficiency to convert the primary alcohol into carboxylate groups, while both 4 and 6 mmol showed a great capability to oxidize cellulose. Considering the zeta potential measurement (more details in next section), the 4 and 6 mmol sodium hypochlorite oxidized cellulose possessed equal zeta potential value. It means that 4 mmol sodium hypochlorite was efficient and enough to operate the oxidation procedure.

In order to study the effect of oxidation time, the oxidation process was performed at various times (6, 18, and 24 hr). For 6 hr, there were a few changes in zeta potential of oxidized cellulose. At 18 and 24 hr of operation time, the zeta potential of oxidized cellulose showed a significant change, and their values were nearly equal. Thus, this work aimed to oxidizie cellulose for 18 hr to reduce the energy consumption and avoid the depolymerization reaction which possibly occurred as the side reaction during oxidation process. The longer oxidation time would lead to possibilities of cellulose depolymerization. This mechanism lowered the cellulose chain length (aspect ratio), and resulted in a reduction in the mechanical properties.

Another step of studies involved with the mechanical condition for producing cellulose nanofiber. The method using homogenization for 2 min and then sonication for 5 min could not convert oxidized cellulose into cellulose nanofiber. These nanofibers could be produced when the oxidized cellulose was homogenized for 4 min and subsequently sonicated for 10 min. According to Fukuzumi et al [32],

จุฬาลงกรณ์มหาวิทยาลัย
CHULALONGKORN UNIVERSITY

cellulose nanofibril length became shorter when longer disintegration time was applied. As mention earlier, cellulose chain length related to their mechanical properties, the lower in chain length the lower in mechanical properties. For this reason, there was no need to spend time longer than this condition.

Table 4.1 Experimental condition for producing cellulose nanofiber

Method		Nanofiber yield
2 mmol sodium hypochlorite	6 hr	-
	18 hr	-
	24 hr	-
4 mmol sodium hypochlorite	6 hr	-
	18 hr	✓
	24 hr	✓
6 mmol sodium hypochlorite	6 hr	-
	18 hr	✓
	24 hr	✓

Method	Nanofiber yield
2 min homogenization + 5 min sonication	-
4 min homogenization + 10 min sonication	✓

In conclusion, the most suitable condition to oxidize cellulose was to use 4 mmol sodium hypochlorite for 18 hr. Then, the oxidized cellulose was separated into cellulose nanofibers by homogenization for 4 min and sonication for 10 min.

After the disintegration process, the cellulose nanofiber was dispersed in water as displayed in **Fig 4.1**. These suspensions were then heated to evaporate the water. Finally, the white powder of cellulose nanofiber was obtained and stored in a dessicator for further investigation and application.

Figure 4.1 The appearance of cellulose nanofiber suspension in water

4.1.1 Cellulose nanofiber morphologies

The morphologies of cellulose nanofiber were studied using transmission electron microscopy (TEM). **Fig 4.2** revealed TEM images of the obtained cellulose nanofibers, which could be implied that the cellulose nanofibers were successfully produced by oxidation and subsequent mechanical disintegration in

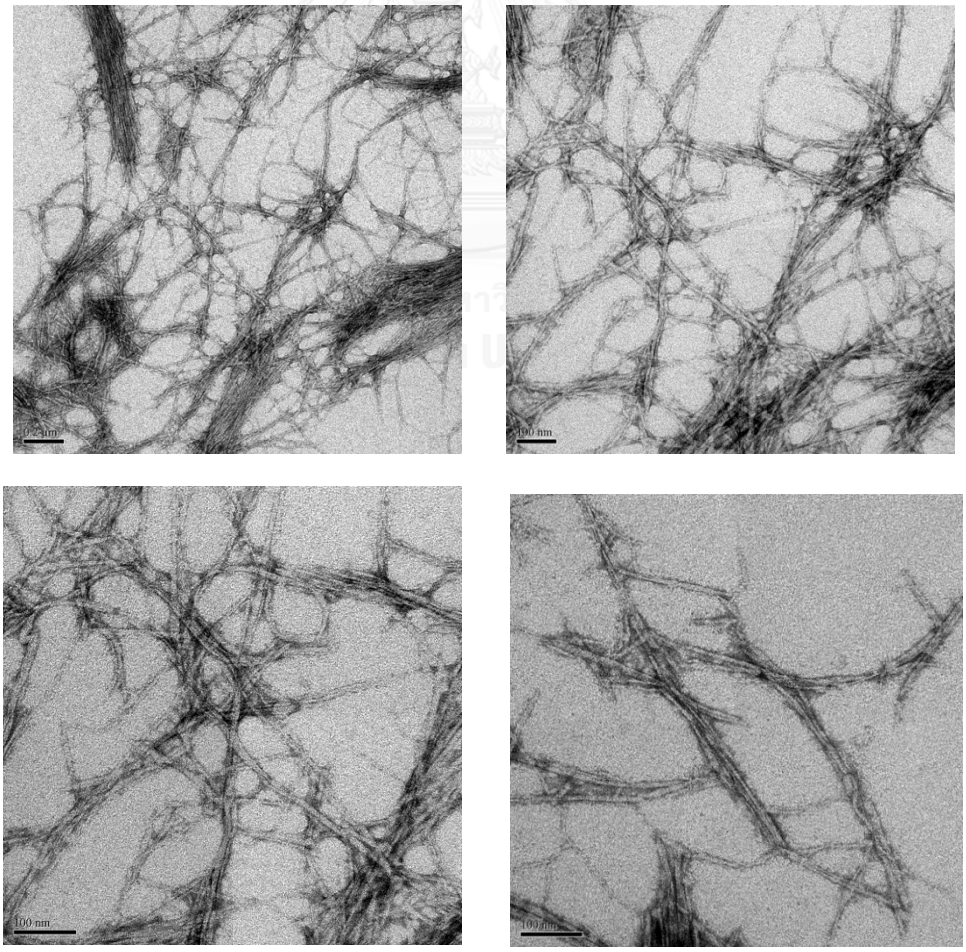

Figure 4.2 TEM images of cellulose nanofiber

water. These cellulose nanofibers possessed diameters in the range of 10–20 nm and at least 1 μm in length. Hence, their aspect ratio was greater than 50, showing a great potential to be utilized as reinforcement.

4.1.2 Chemical structure of cellulose nanofiber

4.1.2.1 Surface characteristic

In this work, the TEMPO mediated oxidation was employed to oxidize extracted sisal cellulose, by converting C6 primary hydroxyls groups to carboxylate groups. These carboxylate groups generated anions on the surface of oxidized cellulose. In order to estimate net electrical charges, zeta potential measurement was utilized to determine the charges on the oxidized cellulose surface. As shown in **Figure 4.3**, zeta potential of oxidized cellulose nanofiber and extracted sisal cellulose (**Figure 4.4**) dispersed in water was about -36 and -18 mV, respectively. The difference in zeta potential indicated that oxidation reaction was successfully occured. The oxidized cellulose had more negative charges, comparing to the extracted cellulose. Consequently, the intense negative charges on the oxidized cellulose surface caused repulsive force, which made it much easier to disintegrate cellulose into the individual cellulose nanofibers.

จุฬาลงกรณ์มหาวิทยาลัย
Chulalongkorn University

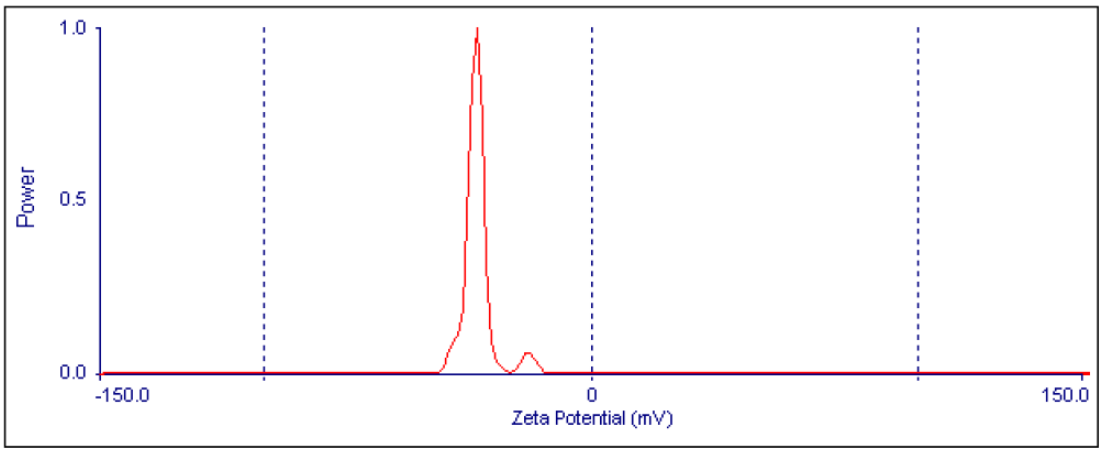

Run	Zeta Potential (mV)	Half Width (mV)
1	-37.22	3.09
2	-34.43	2.79
3	-33.05	2.77
4	-35.32	2.96
5	-33.15	2.85
6	-34.66	2.64
7	-41.58	4.75
8	-43.00	2.66
9	-35.49	3.53
10	-34.79	2.54
Mean	-36.27	3.06
Std. Error	1.08	0.21

จุฬาลงกรณ์มหาวิทยาลัย
Chulalongkorn University

Figure 4.3 Zeta potential of oxidized cellulose nanofiber (0.1 mmol TEMPO, 10 mmol sodium chlorite, 4 mmol sodium hypochlorite for 18 hr)

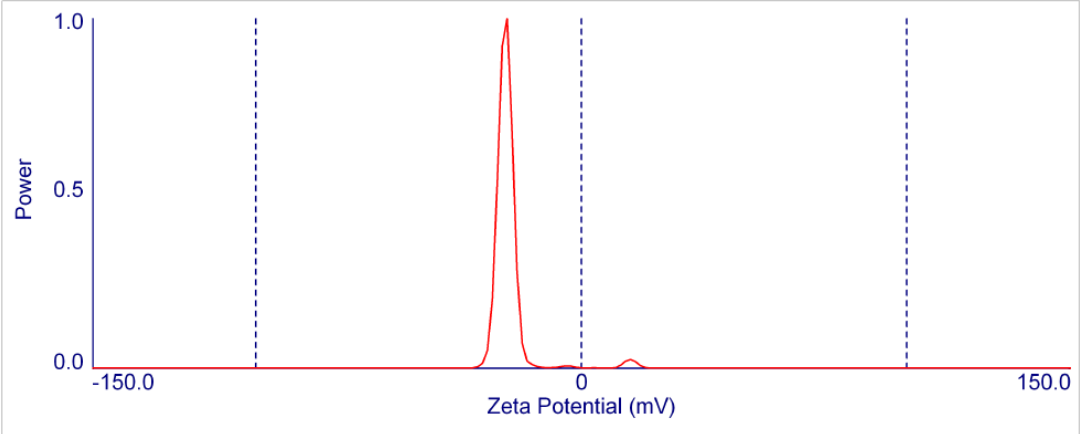

Run	Zeta Potential (mV)	Half Width (mV)
1	-26.01	2.75
2	-21.24	7.74
3	-19.72	2.79
4	-13.87	3.04
5	-12.36	3.41
6	-25.79	4.17
7	-15.39	2.60
8	-12.36	2.65
9	-12.36	4.51
10	-22.76	2.70
Mean	-18.19	3.64
Std. Error	1.76	0.50

Chulalongkorn University

Figure 4.4 Zeta potential of extracted cellulose (2 M NaOH at 60° C for 4 hr, 10% H_2O_2 in 10 % NaOH at 70° C for 70 min)

4.1.2.2 Chemical composition

FTIR analysis was used to investigate the chemical structure of oxidized cellulose. The FTIR spectra of extracted cellulose and oxidized cellulose nanofiber were shown in **Fig 4.5**. The main characteristic peaks of cellulose (i.e. O-H stretching, C-H stretching, and C-H bending at 3400 cm^{-1}, 2900 cm^{-1} , and 1432 cm^{-1}) are presented in both extracted cellulose and oxidized cellulose nanofiber. Nevertheless, there was a significant distinction between oxidized cellulose and extracted cellulose. The intensity of peak at 1609.5 cm^{-1} in the oxidized cellulose spectrum increased after the modification process took place. This region related to the carboxylate COO^- vibration. Similar to the zeta potential measurement, this result confirmed the success in oxidation reaction of extracted cellulose.

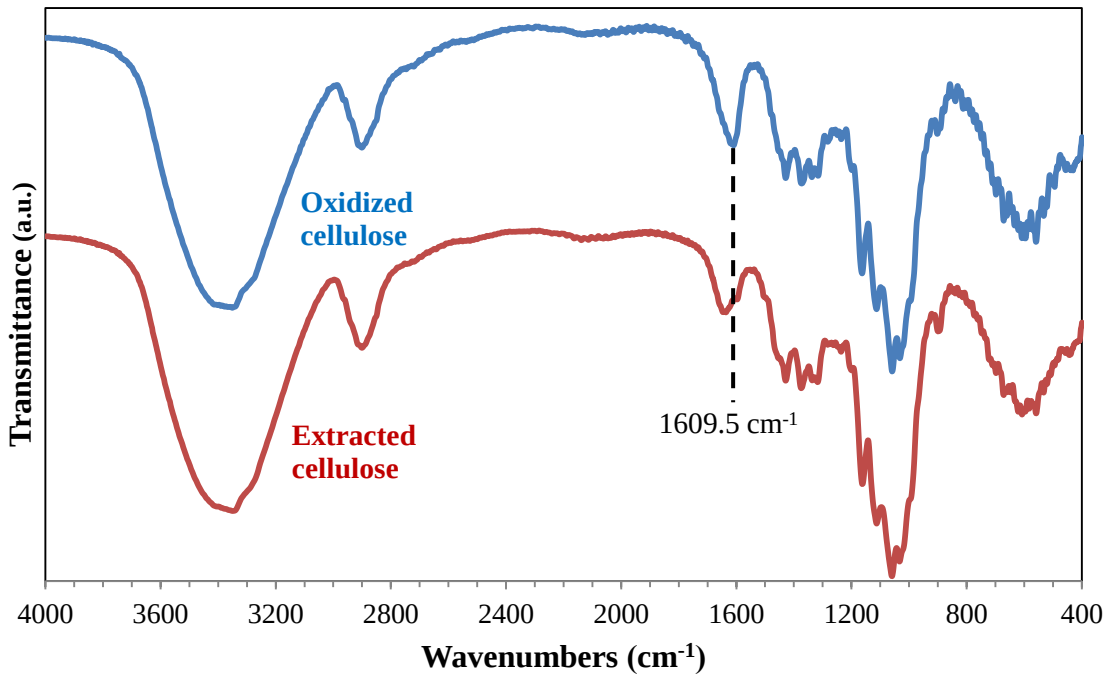

Figure 4.5 FTIR spectra of extracted cellulose and oxidized cellulose nanofiber

4.1.3 Crystalline structure of cellulose nanofiber

X-ray diffraction was utilized to examine the crystalline structure of the cellulose nanofiber. **Fig 4.6** presented the diffraction patterns of oxidized cellulose nanofiber and extracted cellulose. Comparing to the extracted cellulose, the oxidized cellulose nanofiber still exhibited the main characteristic peaks of native cellulose at 2θ = 15°, 16.5°, and 22°, which referred to (1 0 1), (1 0 $\bar{1}$), and (2 0 0) crystallographic planes of the cellulose I lattice, respectively [56]. The crystallinity of cellulose (χ) was calculated following the empirical Segal's equation (Eq.1). The crystallinity of the extracted cellulose was about 70.4%, while that of the oxidized cellulose nanofiber dropped to 62.9%. After oxidation process, the distance between cellulose molecules increased because there were impulsive forces on the cellulose surfaces. Hence, this modification could weaken the intermolecular hydrogen bonds of cellulose structure, and attributed to the reduction in its crystallinity. In addition, the mechanical treatment and side reaction of oxidation procedure probably caused damages to cellulose molecules resulted in decreasing the crystallinity of cellulose structure. Even though there was a lower in the crystallinity, the oxidized cellulose nanofibers still maintained the highly crystalline structure and thus potentially being used as a reinforcement.

จุฬาลงกรณ์มหาวิทยาลัย
Chulalongkorn University

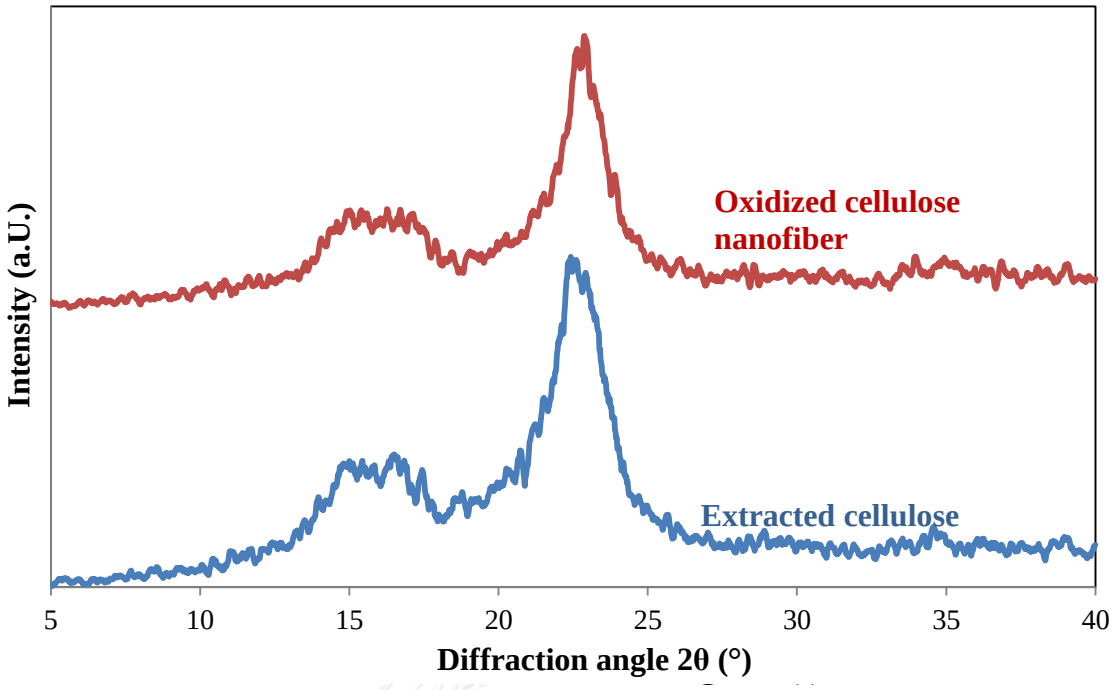

Figure 4.6 X-ray diffraction patterns of extracted cellulose and oxidized cellulose nanofiber

4.1.4 Thermal stability of cellulose nanofiber

Thermal behavior of oxidized cellulose nanofiber and extracted cellulose was shown in **Fig 4.7**. First, the moisture evaporation took place under the range of 40-130 ° C, causing a small weight loss in both oxidized cellulose nanofiber and extracted cellulose. Then, the thermal decomposition of oxidized cellulose nanofiber was beginning at 240 ° C, whereas the thermal degradation of the extracted cellulose initially occurred at 300° C. Comparing to the extracted cellulose, the lower in the decomposition temperature of the oxidized nanofiber was owing to the presence of carboxylate groups which were converted from the C6 primary hydroxyl groups of cellulose molecules through the oxidation process with TEMPO [29]. However, the onset of second degradation of the oxidized cellulose nanofiber at 300° C still existed. This evidence implied that the oxidized cellulose nanofiber still comprised highly crystalline structure of native cellulose.

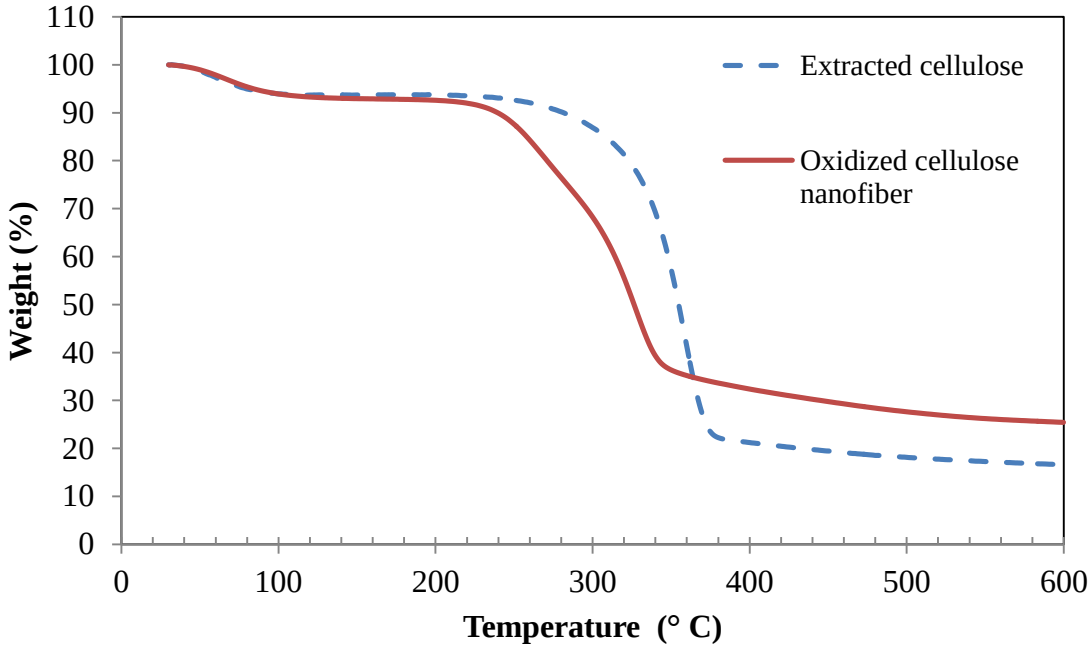

Figure 4.7 TGA thermograms of extracted cellulose and oxidized cellulose nanofiber

จุฬาลงกรณ์มหาวิทยาลัย
Chulalongkorn University

4.2 Characterization of all-cellulose nanocomposite films

The main objective of this research was to find an approach for producing the cellulosic film by solvent casting method. First, the celllose solution was poured into a mold and maintained at room temperature for 8, 12, 24, 48, 72, and 168 hr. During this stage, the solution gradually regenerated and turned into the solid phase. It seemed that the film slowly shrank as time went by. Hence, the small size of film can be produced when kept it for 168 hr.

In order to shorten the experimental time and gain the large sample for testing, the film was kept at ambient temperature for 8 hr. Then, they were washed with water to leach out solvent from the specimens. Finally, they were air-dried at room temperature to evaporate the water and the remaining solvent. The resulted films were wrinkle and crease due to fast evaporation and uneven evaporation rate, thus it was still quite hard to test them.

To solve this problem, drying in a box was used to slow down the evaporation rate, so the films had longer drying time comparing to air dried method. Although this technique could lower the evaporation rate and decrease some wrinkle, the obtained cellulose films still were not smooth enough for testing. By holding all margins of cellulose films with adhesive tapes and drying them in the box, most of the film surface was smooth and ready for further investigation.

จุฬาลงกรณ์มหาวิทยาลัย
Chulalongkorn University

4.2.1 Physical properties

4.2.1.1 Physical appearance

Appearance of the obtained all-cellulose nanocomposite films was exhibited in **Fig 4.8**. The neat cellulose film or SC0 (**Fig 4.8 a**) had a transparent surface and became more translucent when the cellulose nanofibers were added (**Fig 4.8 b, c, d**). The comparison of all sample fims was illustrated in **Fig 4.8**. Clearly, the more reinforcement was filled, the higher films surface was opaque.

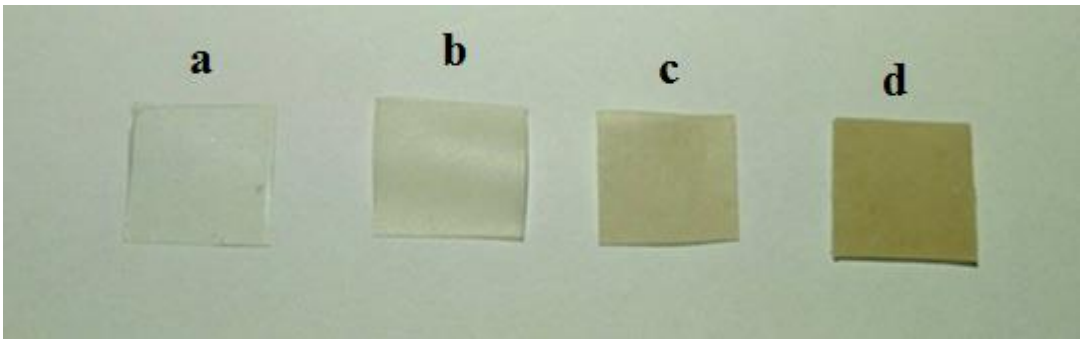

Figure 4.8 The appearance of all-cellulose nanocomposite films (a. SC0; b. SC0.5; c. SC1; d. SC2)

4.2.1.2 All-cellulose nanocomposite films morphologies

The specimens used in the study of morphology were obtained from tensile testing. The fracture surface of all-cellulose nanocomposite films was observed by SEM. **Fig 4.9** showed the SEM micrographs of cross-section for all-cellulose nanocomposites films. Neat cellulose film or SC0 (**Fig 4.9a**) revealed a lamellae-like structure similarly to Duchemin et al. [48] work, in which all-cellulose composite was prepared by partly dissolving microcrystalline cellulose. As shown in **Fig 4.9b**, when adding a few reinforcements, the composite film with 0.5% reinforcement content (SC0.5) still exhibited lamellae-like structure. The reinforcement was embedded and well dispersed in the matrix, showing a good compatibility between matrix and fillers. However, the addition of reinforcement content at 1 % or greater (SC1 and SC2) made the film surface became rougher as the number of cellulose nanofibers further enhanced in the composites (**Fig 4.9c and d**).

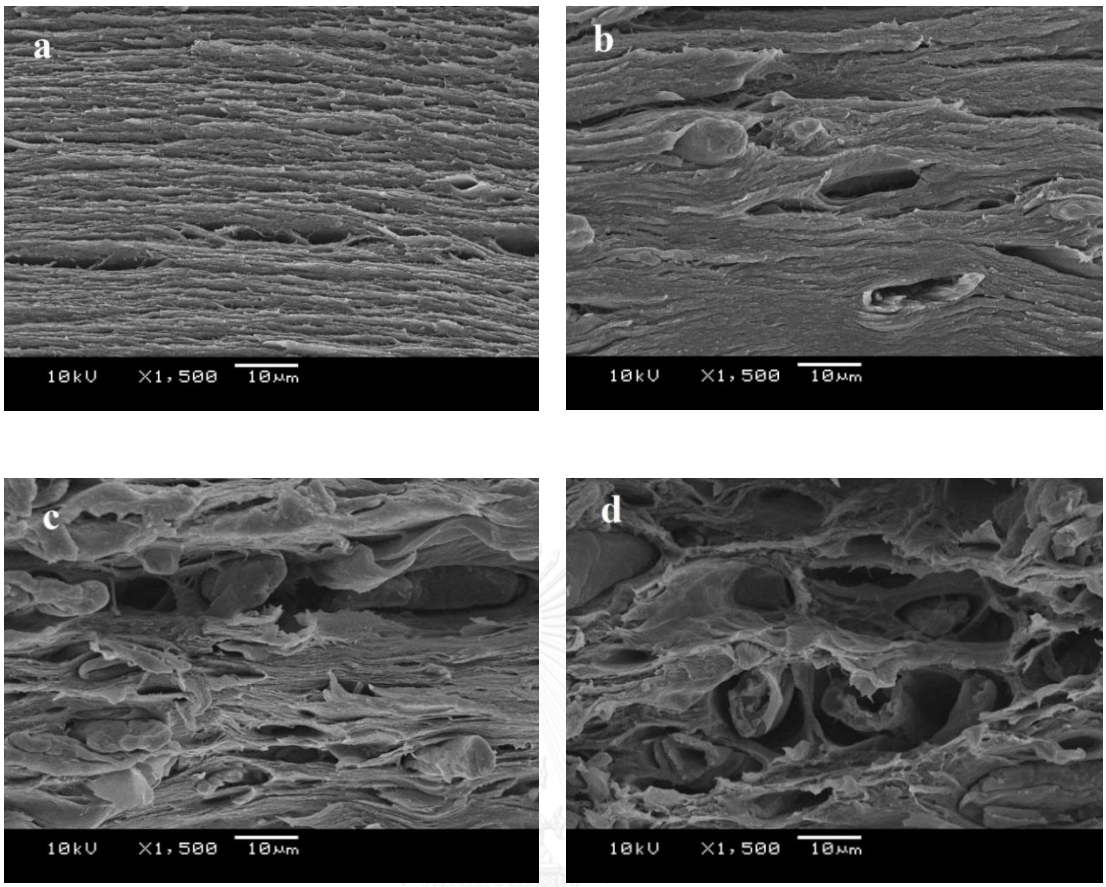

Figure 4.9 SEM images of cross-section for all-cellulose nanocomposite films. (a. SC0; b. SC0.5; c. SC1; d. SC2)

จุฬาลงกรณ์มหาวิทยาลัย
CHULALONGKORN UNIVERSITY

Owing to the high load of fillers as well as the aggregation of reinforcements, the phase separation occurred. This indicated that the poor compatibility arose when high amount of reinforcements was added into the cellulose matrix. These results were in good agreement to tensile properties of the sisal nanocomposite films as will be discussed later.

4.2.1.3 Crystallinity

The crystallinity of the nanocomposite films was examined by wide angle x-ray diffraction. The diffraction patterns of the samples were displayed in **Fig 4.10**. The degree of crystallinity was estimated using Segal's equation (**Eq.1**) and was then summarized in **Table 4.2**. Neat cellulose film or SC0 had the lowest degree

of crystallinity. In dissolution process, the sisal cellulose was supposed to be fully dissolved; however, since some crystalline structure still existed, so it took a week to dissolve the film. This could be attributed to the regeneration process, some crystalline would recrystallize. In addition, it might be that the cellulose did not turn into the fully amorphous structure.

When the cellulose nanofibers were combined into the cellulose films, these highly crystalline reinforcements increased the degree of crystallinity of the nanocomposite films. Besides, the cellulose nanofibers probably act as nucleating agent. This phenomenon also provided a higher degree of crystallinity to the nanocomposite film. The total percent of crystallinity depended on reinforcement ratio in nanocomposite film that upon increasing the amount of cellulose nanofibers, the degree of crystallinity of the nanocomposite films was continuously enhanced. For example, SC2 film obviously exhibited cellulose nanofiber's characteristic peak compared to the neat cellulose film at 2θ = 22°.

Table 4.2 Degree of crystallinity of all-cellulose nanocomposite films

Samples	Degree of crystallinity (%)
SC0	24.87
SC0.5	30.53
SC1	51.73
SC2	64.74

จุฬาลงกรณ์มหาวิทยาลัย
Chulalongkorn University

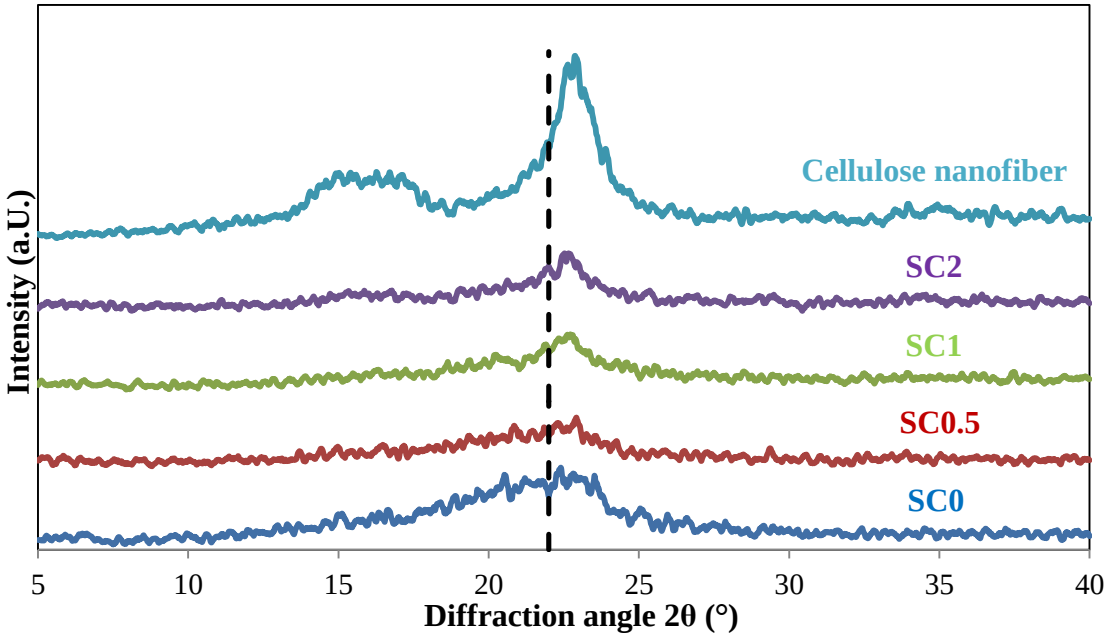

Figure 4.10 X-ray diffraction patterns of all-cellulose nanocomposite films

4.2.1.4 Water uptake behavior

The water uptake behavior of all-cellulose nanocomposite films was followed according to the ASTM D 570 standard. **Fig 4.11** showed % water absorption of all cellulosic films. In the early stage of this experiment, the nanocomposite films quickly absorbed water, and the % water absorption was close to its maximum value within 4 hr from the beginning. After 8 hr of immersion, the film samples eventually approached an equilibrium state. Hence, the water absorption value of the nanocomposite films became stable until the experiment ended.

The % water absorption was calculated using Eq.2 (**section 3.4.2.1.3**). The estimated values of % water absorption for SC0, SC0.5, SC1, and SC2 films were approximately 202, 203, 163, and 150, respectively. The hydrophilicity of the film samples reduced when the content of reinforcement enhanced. This could be attributed to the increasing of the crystalline region. In general, vapor or water is commonly penetrated into the cellulose through the amorphous phase. From the

crystallinity investigation, the insertion of highly crystalline cellulose nanofiber into the matrix declined the total amounts of amorphous region and resulted in lower water uptake of the nanocomposite film.

However, there was a difference for SC0.5 film. The % water absorption at equilibrium was still the same as SC0 film even though the reinforcement was filled. It could be suggested that the small volume of cellulose nanofibers along with high compatibility between matrix and reinforcement made the SC0.5 film become more homogenous than the SC1 and SC2 films. Consequently, SC0.5 film had the hydrophilic property like SC0 or neat cellulose film.

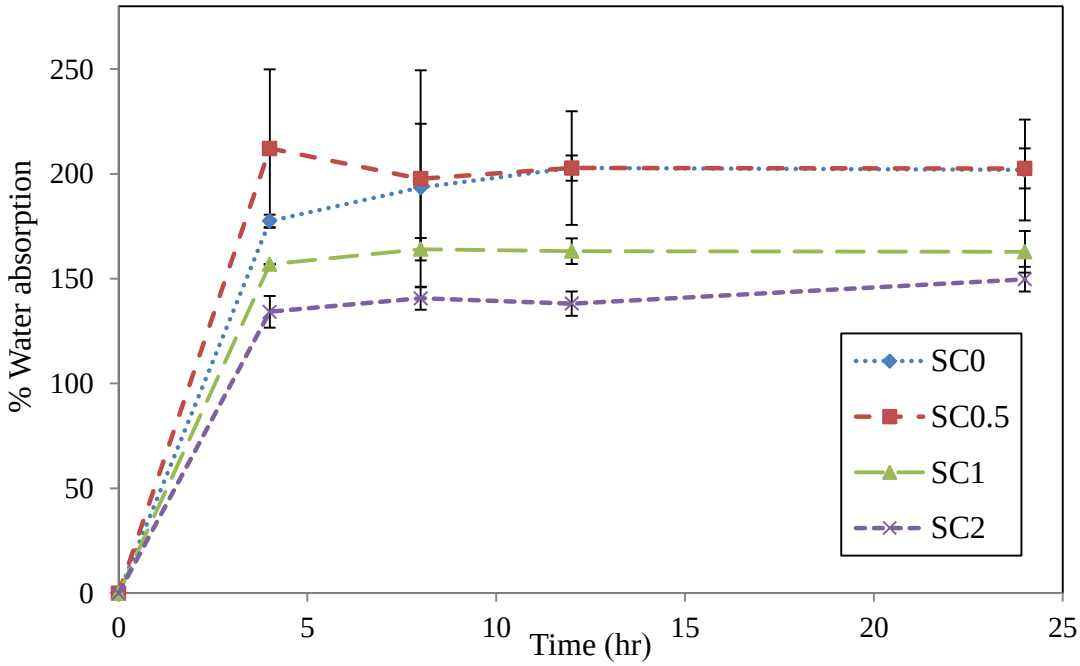

Figure 4.11 % water absorption of all-cellullose nanocomposite films

4.2.2 Tensile properties

Mechanical testing of all-cellulose nanocomposites film was operated according to the ASTM D 882 standard. The nanocomposite films characteristic was illustrated through the stress-strain curves in **Fig 4.12**. The original cellulose or SC0

film exhibited brittle behavior, possessing high Young's modulus (high-stress but low-strain). The incorporation of cellulose nanofibers into SC0 film provided the ductile behavior to them. Although there was some decrease in stress, the strain value of the nanocomposite film with 0.5 % reinforcement content was greatly increased. Thus, the total energy requirement for breaking the SC0.5 films increased and showed that they were tougher comparing with the neat cellulose film. It was different for SC1. Even though the addition of cellulose nanofiber content at 1% still raised the strain of the nanocomposite film, the large declining in tensile strength was leading to the reduction in overall energy. This means that the film was weakened when the aggregation of reinforcement took place, as evidenced by SEM analysis. It was getting worse if the reinforcement was continuously added while the aggregation occurred. In case of SC2, this nanocomposite film had both low tensile strength and elongation at break value. Among all of the samples, SC2 obviously showed the lowest mechanical properties.

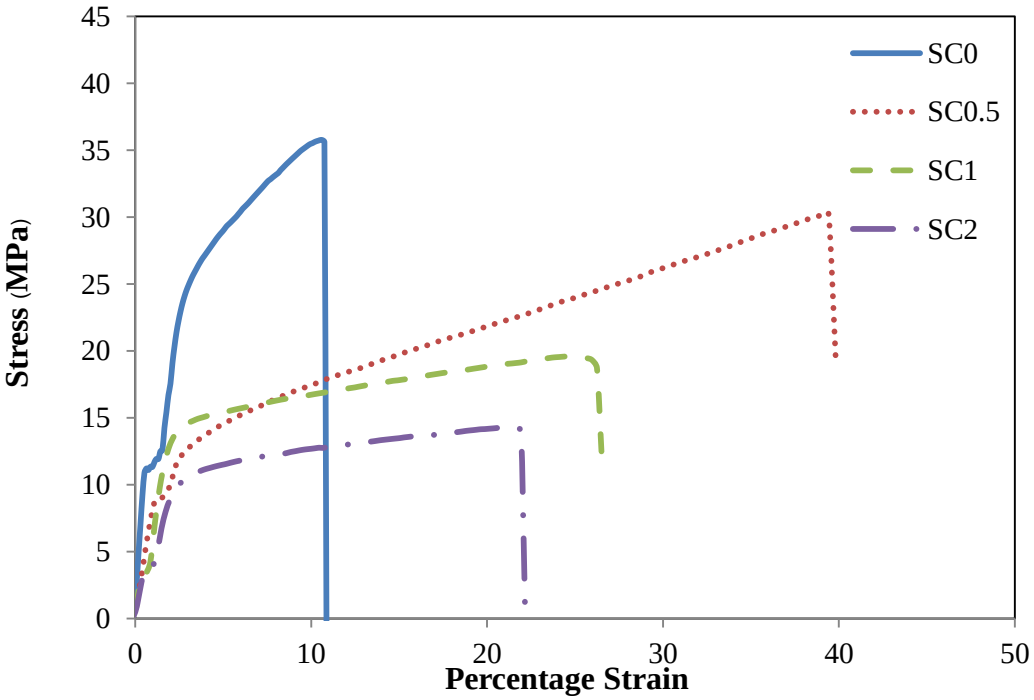

Figure 4.12 Stress-strain curves of the all-cellulose nanocomposite films

The measurement and estimation of mechanical properties were presented in **Table 4.3**. A neat cellulosic film possessed the highest tensile strength around 40 MPa, but had a low elongation at break (11%). By adding the cellulose nanofibers to the neat cellulose film for 0.5% (w/v), the tensile strength of the composite film reduced from 40.30 to 29.06 MPa, while the elongation at break considerably increased from 11% to 37%. From the calculation of the area under the stress-strain curves, it can be indicated that SC0.5 film (45.43 $\times 10^{-2}$ J) was tougher than SC0 film (11.25 $\times 10^{-2}$ J). Nevertheless, the combination of 1 and 2 % reinforcement content with the cellulose matrix resulted in different way. Comparing to SC0.5 film, both tensile strength and elongation at break were decreased; however, their elongation at break was still greater than that of the neat cellulosic film. This could be ascribed to an aggregation of cellulose nanofibers. Due to their extremely high surface areas, cellulose nanofibers easily aggregated whenever a high amount of nanofillers was added. This event created phase separation and caused failure points in the composites. Moreover, as discussed earlier in morphological study that the poor compatibility between matrix and reinforcement could be occurred for SC1 and SC2 films. Thus, it was leading to the insufficient stress transfer and lowered the mechanical properties of the composite films. These results are in good agreement with the work reported by Zhao et al [53].

จุฬาลงกรณ์มหาวิทยาลัย
Chulalongkorn University

Table 4.3 Mechanical properties of all-cellulose nanocomposite films

Samples	Tensile strength (MPa)	Elongation at break (%)	Energy absorption (J) $\times 10^{-2}$
SC0	40.30±4.53	10.85±1.41	11.25±2.32
SC0.5	29.06±3.52	37.40±4.64	45.43±9.79
SC1	20.05±2.20	22.39±6.95	40.88±19.35
SC2	11.96±1.68	15.79±7.30	18.20±11.90

4.2.3 Thermal properties

The thermal degradation characteristic of all-cellulose nanocomposite films was shown in **Fig 4.13**. The two major stages presented for all specimens. The first one was a little weight loss in the temperature range of 40-130° C. The evaporation of moisture from the film samples took place in this stage. The variation of water volatilization in all cellulose films occurred from their difference in reinforcement content. SC0 had the highest weight loss (8.78%) in this temperature range, followed by SC0.5 (7.23%), SC1 (4.91%), and SC2 (4.78%), respectively. As discussion in water uptake behavior section, this is because neat cellulose film or SC0 possessed the greatest amount of amorphous region, which is the area for water to enter into the cellulose structure. Thus, the addition of highly crystalline reinforcement could reduce the amorphous part of the cellulose film, and decreased the total moisture content of the film.

Another stage of mass loss was thermal decomposition of the cellulose structure. The onset of decomposition temperature (T_d^{onset}) and degradation temperature at 50% solid residual ($T_d^{50\%}$) of all samples were listed in **Table 4.4**. T_d^{onset} of the all-cellulose nanocomposite film had the same manner to the tensile properties that it was higher than the neat cellulose film when the reinforcement was mixed. However, the addition of high volume reinforcements (more than 0.5%) could cause the phase separation, leading to a drop in T_d value.

In case of $T_d^{50\%}$, it had different behavior. The increasing of cellulose nanofibers led to an improvement in the $T_d^{50\%}$ value. Comparing to the neat cellulose film, $T_d^{50\%}$ of SC1 and SC2 was still higher even though the phase separation appeared. It was supposed that the $T_d^{50\%}$ of the composite was risen from the cellulose nanofibers, which had high thermal stability owing to its greatly crystalline structure. These cellulose nanofibers possessed the $T_d^{50\%}$ value around 326° C, as showed in **Fig 4.7**.

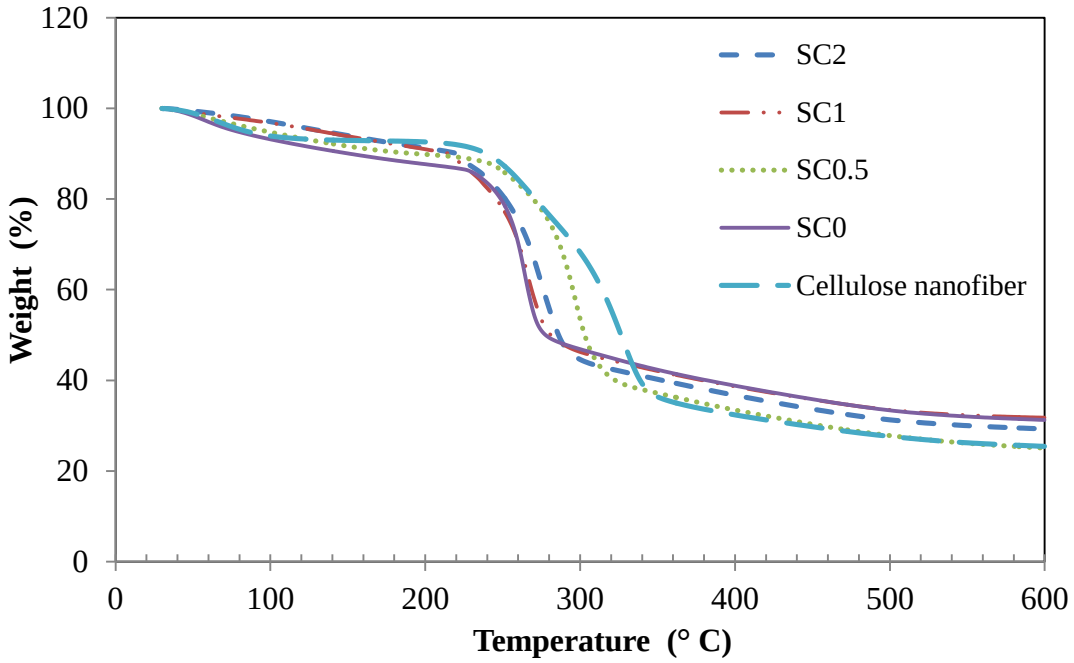

Figure 4.13 TGA thermograms of all-cellulose nanocomposite films

Table 4.4 Thermal properties of all-cellulose nanocomposite films

Samples	Moisture evaporation (%)	T_d^{onset} (° C)	$T_d^{50\%}$ (° C)
SC0	8.78	262	277
SC0.5	7.23	270	303
SC1	4.91	244	281
SC2	4.78	249	286

จุฬาลงกรณ์มหาวิทยาลัย
Chulalongkorn University

CHAPTER V
CONCLUSIONS

5.1 Conclusions

In this study, extracted sisal cellulose was oxidized using TEMPO/ NaClO/ $NaClO_2$ system, and subsequently disintegrated by homogenization and sonication in water. The obtained cellulose nanofibers were then used as reinforcement in all-cellulose composite films. The matrix of the composite films was prepared by dissolving sisal cellulose in LiCl/DMAc solution. Besides, the investigation of proper conditions for preparation of cellulose nanofiber and all-cellulose nanocomposite films was also studied. The characterization of cellulose nanofiber and the effects of cellulose nanofiber content on mechanical properties, physical properties, and thermal properties of the all-cellulose nanocomposite films were examined. All of these results are concluded below:

Part I: Characterization of cellulose nanofiber

- The proper condition for preparing cellulose nanofiber was to oxidize sisal cellulose with 4 mmol sodium hypochlorite, 0.1 mmol TEMPO, and 10 mmol sodium chlorite for 18 hr. A decreasing in zeta potential values and an increasing of peak intensity at 1609.5 cm^{-1} (carboxylate vibration) in the FTIR spectrum proved the success in oxidation. Physical appearance of the obtained cellulose nanofiber is a white powder. A morphology of cellulose nanofiber observed by TEM revealed the nanofibers having diameters in the range of 10–20 nm and at least 1 μm in length.

- The diffraction patterns of cellulose nanofiber exhibited the main characteristic peaks of native cellulose at 2θ = 15°, 16.5°, and 22°, respectively. Comparing to extracted cellulose, there was no change in crystalline structure. However, the crystallinity of cellulose nanofiber was slightly decreased (from 70.4% to 62.9%) due to the oxidation and mechanical procedure.

- The thermogravimetric curve of cellulose nanofiber showed that the initial decomposition temperature was dropping from 300° C to 240° C owing to the existence of carboxylate group at C6. Nevertheless, the mass decomposition at 300° C still existed, indicating that cellulose nanofiber consisted of highly crystalline structure.

Part II: Characterization of all-cellulose nanocomposite films

- Shape of the all-cellulose nanocomposite films was depended on their molds. The surface of the neat cellulose film was transparent and had become more translucent when greater amount of the cellulose nanofibers was added into the composite films.

- SEM image of the neat cellulose film exhibited a lamellae-like morphology. This structure still maintained although the 0.5% cellulose nanofiber content was filled. When the cellulose nanofiber content was over 1%, the rough surface was observed, and became rougher as the number of cellulose nanofibers increased. Moreover, the high cellulose nanofibers

content could cause the aggregation, and leading to the phase separation. This phenomenon showed that the incompatibility increased when high amount of cellulose nanofiber was applied into the composite films.

- The insertion of highly crystalline cellulose naofiber into the composite films increased the degree of crystallinity of the all-cellulose nanocomposite films. Thus, the nanocomposite with 2 % reinforcement content showed the highest degree of crystallinity, approximately 64.74%.

- The hydrophilicity of the all-cellulose nanocomposite films was lowered with an increasing of the cellulose nanofiber content because the addition of cellulose nanofiber decreased the amorphous region, which was the area for water to penetrate into the cellulose. Hence, the % water absorption of the composite film with 2 % reinforcement content was reduced from 202 to 150.

จุฬาลงกรณ์มหาวิทยาลัย
Chulalongkorn University

- The neat cellulose films showed brittle characteristic, possessing the highest tensile strength around 40 MPa but low elongation at break (11%). The incorporation of cellulose for 0.5% (w/v) caused a little decreasing in tensile strength from 40.30 to 29.06 MPa while the elongation at break greatly increased from 11% to 37%. However, the addition of 1 and 2 % cellulose nanofiber content led to the different outcome when comparing to the neat cellulose film. It was found that the tensile strength was decreased, in the meantime the elongation at break was also declined but the value was still higher than that of the neat cellulose film. The reduction in

tensile strength was attributed to an aggregation of cellulose nanofibers.

- The onset of decomposition temperature (T_d^{onset}) for the all-cellullose nanocomposite films performed the same behavior as the mechanical properties that it had the highest value when adding cellulose nanofiber for 0.5 % (w/v). On the other hand, there was a different manner for degradation temperature at 50% solid residual ($T_d^{50\%}$). The $T_d^{50\%}$ value of the composite film still increased although the phase separation took place because of the high thermal properties of the reinforcement.

5.2 Recommendation

- In order to increase the reproducibility, dissolving the sisal cellulose in LiCl/DMAc solution should be shorten by studying the relationship between the time that used for dissolving the cellulose and the degree of crystallinity for the neat cellulose film. If the degree of crystallinity becomes a constant value within 7 days, the preparation time for cellulose solution will be successfully decreased.

- It is well known that aspect ratio of the reinforcement affects the mechanical properties. So, the variation of the disintegration conditions (e.g. time, speed, apparatus) may provide better results.

- Due to the aggregation of the reinforcement, there was a limitation to fill higher amount of cellulose nanofiber. Some fillers should be applied to prevent the aggregation. As a result, the composite films could take more cellulose nanofiber and thus improve their mechanical as well as thermal properties.

จุฬาลงกรณ์มหาวิทยาลัย
Chulalongkorn University

REFERENCES

[1] Satyamurthy, P. and Vigneshwaran, N. A novel process for synthesis of spherical nanocellulose by controlled hydrolysis of microcrystalline cellulose using anaerobic microbial consortium. Enzyme and Microbial Technology 52(1) (2013): 20-25.

[2] Yano, H. and Nakahara, S. Bio-composites produced from plant microfiber bundles with a nanometer unit web-like network. Journal of Materials Science 39(5) (2004): 1635-1638.

[3] Abdul Khalil, H.P.S., et al. Production and modification of nanofibrillated cellulose using various mechanical processes: A review. Carbohydrate Polymers 99 (2014): 649-665.

[4] Jiang, F. and Hsieh, Y.-L. Chemically and mechanically isolated nanocellulose and their self-assembled structures. Carbohydrate Polymers 95(1) (2013): 32-40.

[5] Dufresne, A. Nanocellulose: a new ageless bionanomaterial. Materials Today 16(6) (2013): 220-227.

[6] Alemdar, A. and Sain, M. Isolation and characterization of nanofibers from agricultural residues – Wheat straw and soy hulls. Bioresource Technology 99(6) (2008): 1664-1671.

[7] López-Rubio, A., et al. Enhanced film forming and film properties of amylopectin using micro-fibrillated cellulose. Carbohydrate Polymers 68(4) (2007): 718-727.

[8] Saito, T. and Isogai, A. TEMPO-Mediated Oxidation of Native Cellulose. The Effect of Oxidation Conditions on Chemical and Crystal Structures of the Water-Insoluble Fractions. Biomacromolecules 5(5) (2004): 1983-1989.

[9] Huber, T., Müssig, J., Curnow, O., Pang, S., Bickerton, S., and Staiger, M. A critical review of all-cellulose composites. Journal of Materials Science 47(3) (2012): 1171-1186.

Chulalongkorn University

[10] Nishino, T., Matsuda, I., and Hirao, K. All-Cellulose Composite. Macromolecules 37(20) (2004): 7683-7687.

[11] Somsub, S. and Aht-Ong, D.D. Physical, Mechanical, and Thermal Properties of Sisal Cellulose Biocomposite Films. in Advanced Materials Research, pp. 1016-1020: Trans Tech Publ, 2012.

[12] Medronho, B. and Lindman, B. Brief overview on cellulose dissolution/regeneration interactions and mechanisms. Adv Colloid Interface Sci 222 (2015): 502-8.

[13] Giri, J. and Adhikari, R. A Brief review on extraction of nanocellulose and its application. 2012 9 (2012): 7.

[14] Lavoine, N., Desloges, I., Dufresne, A., and Bras, J. Microfibrillated cellulose - its barrier properties and applications in cellulosic materials: a review. Carbohydr Polym 90(2) (2012): 735-64.

[15] Abdul Khalil, H.P.S., Bhat, A.H., and Ireana Yusra, A.F. Green composites from sustainable cellulose nanofibrils: A review. Carbohydrate Polymers 87(2) (2012): 963-979.

[16] Kim, J.-H., et al. Review of nanocellulose for sustainable future materials. International Journal of Precision Engineering and Manufacturing-Green Technology 2(2) (2015): 197-213.

[17] Jonoobi, M., et al. Different preparation methods and properties of nanostructured cellulose from various natural resources and residues: a review. Cellulose 22(2) (2015): 935-969.

[18] DODSON, B. Wood pulp extract stronger than carbon fiber or Kevlar 2012. [March 16]

[19] Saito, T., Hirota, M., Tamura, N., and Isogai, A. Oxidation of bleached wood pulp by TEMPO/NaClO/NaClO2 system: effect of the oxidation conditions on carboxylate content and degree of polymerization. Journal of Wood Science 56(3) (2010): 227-232.

[20] Iwamoto, S., Kai, W., Isogai, T., Saito, T., Isogai, A., and Iwata, T. Comparison study of TEMPO-analogous compounds on oxidation efficiency of wood

cellulose for preparation of cellulose nanofibrils. Polymer Degradation and Stability 95(8) (2010): 1394-1398.

[21] Saito, T., Nishiyama, Y., Putaux, J.-L., Vignon, M., and Isogai, A. Homogeneous Suspensions of Individualized Microfibrils from TEMPO-Catalyzed Oxidation of Native Cellulose. Biomacromolecules 7(6) (2006): 1687-1691.

[22] Saito, T., Kimura, S., Nishiyama, Y., and Isogai, A. Cellulose Nanofibers Prepared by TEMPO-Mediated Oxidation of Native Cellulose. Biomacromolecules 8(8) (2007): 2485-2491.

[23] Puangsin, B., Fujisawa, S., Kuramae, R., Saito, T., and Isogai, A. TEMPO-Mediated Oxidation of Hemp Bast Holocellulose to Prepare Cellulose Nanofibrils Dispersed in Water. Journal of Polymers and the Environment 21(2) (2013): 555-563.

[24] Fujisawa, S., Isogai, T., and Isogai, A. Temperature and pH stability of cellouronic acid. Cellulose 17(3) (2010): 607-615.

[25] Okita, Y., Saito, T., and Isogai, A. Entire Surface Oxidation of Various Cellulose Microfibrils by TEMPO-Mediated Oxidation. Biomacromolecules 11(6) (2010): 1696-1700.

[26] Shinoda, R., Saito, T., Okita, Y., and Isogai, A. Relationship between Length and Degree of Polymerization of TEMPO-Oxidized Cellulose Nanofibrils. Biomacromolecules 13(3) (2012): 842-849.

[27] Iwamoto, S., Kai, W., Isogai, A., and Iwata, T. Elastic Modulus of Single Cellulose Microfibrils from Tunicate Measured by Atomic Force Microscopy. Biomacromolecules 10(9) (2009): 2571-2576.

[28] Saito, T., Kuramae, R., Wohlert, J., Berglund, L.A., and Isogai, A. An ultrastrong nanofibrillar biomaterial: the strength of single cellulose nanofibrils revealed via sonication-induced fragmentation. Biomacromolecules 14(1) (2013): 248-53.

[29] Fukuzumi, H., Saito, T., Iwata, T., Kumamoto, Y., and Isogai, A. Transparent and High Gas Barrier Films of Cellulose Nanofibers Prepared by TEMPO-Mediated Oxidation. Biomacromolecules 10(1) (2009): 162-165.

[30] Besbes, I., Vilar, M.R., and Boufi, S. Nanofibrillated cellulose from Alfa, Eucalyptus and Pine fibres: Preparation, characteristics and reinforcing potential. Carbohydrate Polymers 86(3) (2011): 1198-1206.

[31] Puangsin, B., Yang, Q., Saito, T., and Isogai, A. Comparative characterization of TEMPO-oxidized cellulose nanofibril films prepared from non-wood resources. Int J Biol Macromol 59 (2013): 208-13.

[32] Fukuzumi, H., Saito, T., and Isogai, A. Influence of TEMPO-oxidized cellulose nanofibril length on film properties. Carbohydr Polym 93(1) (2013): 172-7.

[33] Isogai, A., Saito, T., and Fukuzumi, H. TEMPO-oxidized cellulose nanofibers. Nanoscale 3(1) (2011): 71-85.

[34] Shibata, I. and Isogai, A. Depolymerization of cellouronic acid during TEMPO-mediated oxidation. Cellulose 10(2) (2003): 151-158.

[35] Saito, T., et al. Individualization of Nano-Sized Plant Cellulose Fibrils by Direct Surface Carboxylation Using TEMPO Catalyst under Neutral Conditions. Biomacromolecules 10(7) (2009): 1992-1996.

[36] Tanaka, R., Saito, T., and Isogai, A. Cellulose nanofibrils prepared from softwood cellulose by TEMPO/NaClO/NaClO(2) systems in water at pH 4.8 or 6.8. Int J Biol Macromol 51(3) (2012): 228-34.

[37] Li, Y., Mai, Y.-W., and Ye, L. Sisal fibre and its composites: a review of recent developments. Composites Science and Technology 60(11) (2000): 2037-2055.

[38] Saxena, M., Pappu, A., Haque, R., and Sharma, A. Sisal Fiber Based Polymer Composites and Their Applications. in Kalia, S., Kaith, B.S., and Kaur, I. (eds.),Cellulose Fibers: Bio- and Nano-Polymer Composites, pp. 589-659: Springer Berlin Heidelberg, 2011.

[39] Faruk, O., Bledzki, A.K., Fink, H.-P., and Sain, M. Biocomposites reinforced with natural fibers: 2000–2010. Progress in Polymer Science 37(11) (2012): 1552-1596.

[40] Ramzy, A., Beermann, D., Steuernagel, L., Meiners, D., and Ziegmann, G. Developing a new generation of sisal composite fibres for use in industrial applications. Composites Part B: Engineering 66 (2014): 287-298.

[41] Campbell, F.C. Structural Composite Materials. Materials Park, Ohio: ASM International, 2010.

[42] Staab, G.H. Introduction to composite materials. (2015): 1-16.

[43] Chung, D.D.L. Composite Materials. in *Science and Applications*, Derby, P.B., Editor. 2010, Springer-Verlag London: www.springer.com. 371.

[44] Agrawal, J.P. Composite Materials. Popular Science & Technology (PST). Defence Research & Development Organisation
Ministry of Defence, Delhi-110 054: DESIDOC, 1990.

[45] Soykeabkaew, N., Arimoto, N., Nishino, T., and Peijs, T. All-cellulose composites by surface selective dissolution of aligned ligno-cellulosic fibres. Composites Science and Technology 68(10-11) (2008): 2201-2207.

[46] Miao, C. and Hamad, W.Y. Cellulose reinforced polymer composites and nanocomposites: a critical review. Cellulose 20(5) (2013): 2221-2262.

[47] Qin, C., Soykeabkaew, N., Xiuyuan, N., and Peijs, T. The effect of fibre volume fraction and mercerization on the properties of all-cellulose composites. Carbohydrate Polymers 71(3) (2008): 458-467.

[48] Duchemin, B.J.C., Newman, R.H., and Staiger, M.P. Structure–property relationship of all-cellulose composites. Composites Science and Technology 69(7-8) (2009): 1225-1230.

[49] Pullawan, T., Wilkinson, A.N., and Eichhorn, S.J. Discrimination of matrix–fibre interactions in all-cellulose nanocomposites. Composites Science and Technology 70(16) (2010): 2325-2330.

[50] Pullawan, T., Wilkinson, A.N., and Eichhorn, S.J. Orientation and deformation of wet-stretched all-cellulose nanocomposites. Journal of Materials Science 48(22) (2013): 7847-7855.

[51] Alcalá, M., González, I., Boufi, S., Vilaseca, F., and Mutjé, P. All-cellulose composites from unbleached hardwood kraft pulp reinforced with nanofibrillated cellulose. Cellulose 20(6) (2013): 2909-2921.

[52] Ghaderi, M., Mousavi, M., Yousefi, H., and Labbafi, M. All-cellulose nanocomposite film made from bagasse cellulose nanofibers for food packaging application. Carbohydr Polym 104 (2014): 59-65.

[53] Zhao, J., et al. Reinforcement of all-cellulose nanocomposite films using native cellulose nanofibrils. Carbohydr Polym 104 (2014): 143-50.

[54] Pullawan, T., Wilkinson, A.N., Zhang, L.N., and Eichhorn, S.J. Deformation micromechanics of all-cellulose nanocomposites: comparing matrix and reinforcing components. Carbohydr Polym 100 (2014): 31-9.

[55] Segal, L., Creely, J., Martin, A., and Conrad, C. An empirical method for estimating the degree of crystallinity of native cellulose using the X-ray diffractometer. Textile Research Journal 29(10) (1959): 786-794.

[56] Abdollahi, M., Alboofetileh, M., Rezaei, M., and Behrooz, R. Comparing physico-mechanical and thermal properties of alginate nanocomposite films reinforced with organic and/or inorganic nanofillers. Food Hydrocolloids 32(2) (2013): 416-424.

จุฬาลงกรณ์มหาวิทยาลัย
Chulalongkorn University

APPENDIX

จุฬาลงกรณ์มหาวิทยาลัย
Chulalongkorn University

VITA

Mister Noppon Somsesta was born in Pattani, Thailand on January 6, 1991. He graduated his Bachelor's Degree of Science in Chemistry (second-class honors) from Faculty of science, Prince of Songkla University in 2013. In that year, he continued his education in the Master Degree Program in Applied Polymer Science and Textile Technology at Department of Materials Science, Faculty of Science, Chulalongkorn University in the first semester of academic year 2013. He eventually completed the Master of Science in Applied Polymer Science and Textile Technology Degree in December 2015.

Publications:

National Presentation

1. N. Somsesta and D. Aht-Ong, 2015. "ALL-CELLULOSE NANOCOMPOSITE FILMS FROM SISAL FIBER", The 10th Conference on Science and Technology For Youths, Bangkok, Thailand, June 19-20, 2015 (poster presentation)

2. N. Somsesta and D. Aht-Ong, 2015. "ALL-CELLULOSE NANOCOMPOSITE FILMS FROM SISAL FIBER", The 41st Congress on Science and Technology of Thailand (STT41), Nakhonratchasima, Thailand, November 6 - 8, 2015 (poster presentation)

International Presentation

1. N. Somsesta and D. Aht-Ong, 2015. "ALL-CELLULOSE NANOCOMPOSITE FILMS FROM SISAL FIBER", The 10th International Symposium in Science and Technology 2015 (ISST 2015), Bangkok, Thailand, August 31 - September 2, 2015 (poster presentation)